Chemical Composition and Hydrolysis of Organic Nitrate Aerosol Formed from Hydroxyl and Nitrate Radical Oxidation of α-pinene and β-pinene

Masayuki Takeuchi[1] and Nga L. Ng[2,3*]

[1]School of Civil and Environmental Engineering, Georgia Institute of Technology, Atlanta, Georgia, 30332, USA

[2]School of Chemical and Bimolecular Engineering, Georgia Institute of Technology, Atlanta, Georgia, 30332, USA

[3]School of Earth and Atmospheric Sciences, Georgia Institute of Technology, Atlanta, Georgia, 30332, USA

[*]Corresponding author: ng@chbe.gatech.edu

Keywords

Aerosol, chemical composition, hydrolysis, monoterpenes, organic nitrate, hydroxyl and nitrate radical oxidation

Abstract

Atmospheric organic nitrate (ON) is thought to play a crucial role in the formation potential of ozone and aerosol, which are the leading air pollutants of concern across the world. Limited fundamental knowledge and understanding of the life cycles of ON currently hinders the ability to quantitatively assess its impacts on the formation of these pollutants. Although hydrolysis is currently considered as an important loss mechanism of ON based on prior field measurement studies, this process for atmospherically relevant ON has not been well constrained by fundamental laboratory studies. In this comprehensive study, we investigated the chemical composition and hydrolysis process of particulate ON ($_{p}$ON) formed from the oxidation of α-pinene and β-pinene by hydroxyl (OH·) and nitrate radicals (NO_3·). For $_{p}$ON that undergoes hydrolysis, the hydrolysis lifetime is determined to be no more than 30 min for all systems explored. This is significantly shorter than those reported in previous chamber studies (i.e., 3-6 h) but is consistent with the reported lifetime from bulk solution measurement studies (i.e., 0.02-8.8 h). The discrepancy appears to stem from the choice of proxy used to estimate the hydrolysis lifetime. The measured hydrolyzable fractions of $_{p}$ON (F_H) in the α-pinene+OH·, β-pinene+OH·, α-pinene+NO_3·, and β-pinene+NO_3· systems are 23-32, 27-34, 9-17, and 9-15 %, respectively. While a very low F_H for the NO_3· oxidation system is expected based on prior studies, F_H for the OH· oxidation system is surprisingly lower than predicted in past studies. Overall, the hydrolysis lifetime as well as F_H obtained in this study serve as experimentally constrained parameters that are required in regional and global chemical transport models to accurately evaluate the impacts of ON on nitrogen budget and formation of ozone and aerosol.

1. Introduction

The oxidation of biogenic volatile organic compounds (BVOC) by ozone (O_3), hydroxyl radicals ($OH\cdot$) and nitrate radicals ($NO_3\cdot$) is a major source of secondary organic aerosol (SOA) globally (Kanakidou et al., 2005; Goldstein and Galbally, 2007; Spracklen et al., 2011). Many studies have pointed to the synergistic effects of anthropogenic emissions on biogenic SOA formation in the atmosphere (Weber et al., 2007; Carlton et al., 2010; Hoyle et al., 2011; Shilling et al., 2013; Xu et al., 2015a; Shrivastava et al., 2019). The oxidation of BVOC in environments with anthropogenic NO_x emissions is an important mechanism for coupled biogenic-anthropogenic interactions. In the presence of NO_x, the oxidation of BVOC can lead to the formation of organic nitrate (ON), a large component of reactive oxidized nitrogen. Results from ambient field measurements have revealed the ubiquitous presence of particulate ON ($_pON$), where it contributes to a large fraction of submicron organic aerosol at different sites worldwide (Fry et al., 2013; Xu et al., 2015b; Liu et al., 2012a; Rollins et al., 2012; Rollins et al., 2013; Lee et al., 2016; Kiendler-Scharr et al., 2016; Ng et al., 2017). These findings highlights the importance to understand the formation and fates of ON to accurately evaluate its roles in NO_x recycling, O_3, and SOA formation.

Monoterpenes ($C_{10}H_{16}$) is a major class of BVOC, with annual emissions of 157-177 Tg C yr^{-1} (Guenther et al., 2012). Laboratory studies have demonstrated that the $NO_3\cdot$ oxidation of monoterpenes leads to a substantial formation of ON and SOA, with ON yields up to ~70% (Wangberg et al., 1997; Berndt and Boge, 1997; Griffin et al., 1999; Hallquist et al., 1999; Spittler et al., 2006; Fry et al., 2009; Fry et al., 2014; Boyd et al., 2015; Nah et al., 2016; Boyd et al., 2017; Slade et al., 2017; Claflin and Ziemann, 2018). For photooxidation of monoterpenes in the presence of NO_x, ON yields as high as 26% have been reported for α-pinene (Noziere et al., 1999; Aschmann et al., 2002; Rindelaub et al., 2015). Monoterpene emissions do not depend strongly on light and typically continue at night, making them important ON and SOA precursors at any times of the day (daytime and nighttime) and throughout the year (different seasons). It has been shown that monoterpene-derived ON is prevalent in areas where there are substantial biogenic-anthropogenic interactions and oxidation of monoterpenes contributes to a large fraction of SOA observed

62 in the Southeastern U.S. (Xu et al., 2015a; Xu et al., 2015b; Lee et al., 2016; Zhang et al., 2018; Xu et al.,
63 2018a).

64 One of the largest uncertainties in our understanding of monoterpene ON chemistry is the extent to
65 which ON act as a permanent sink versus temporary reservoir of NO_x (Takeuchi and Ng, 2018). This would
66 depend on the fates of ON as they can either retain or release NO_x upon further reactions. Once formed,
67 gas-phase ON can undergo photolysis or OH· oxidation to release NO_x or partition into the particle phase.
68 $_p$ON in turn can undergo further chemistry to release NO_x or hydrolyze in the particle phase to form nitric
69 acid (HNO_3). Further, ON and HNO_3 can be removed via dry and wet deposition. One important reaction
70 of ON in the particle phase is hydrolysis in the presence of aerosol water, which is a mechanism for NO_x
71 loss (Day et al., 2010; Russell et al., 2011). Studies with bulk solutions showed that particle-phase
72 hydrolysis of tertiary nitrate is fast with a lifetime of minutes, while primary and secondary nitrate is stable
73 (Darer et al., 2011; Hu et al., 2011). However, the hydrolysis of $_p$ON in aerosol water is largely
74 unconstrained. Results from field and modeling studies suggested a $_p$ON lifetime of a few hours (Pye et al.,
75 2015; Lee et al., 2016; Fisher et al., 2016; Zare et al., 2018). A few recent laboratory chamber studies
76 elicited a complex picture where $_p$ON formed from photochemical oxidation and NO_3· oxidation of
77 monoterpenes appear to experience different magnitudes of hydrolysis (Boyd et al., 2015; Rindelaub et al.,
78 2015; Bean and Hildebrandt Ruiz, 2016; Boyd et al., 2017), likely due to the difference in the relative
79 amount of primary, secondary, and tertiary nitrate in these oxidation systems. Overall, there are very limited
80 studies on the further evolutions of ON produced from the oxidation of monoterpenes.

81 Here, we present results from a laboratory chamber study on the chemical composition and
82 hydrolysis process of $_p$ON formed from oxidation of α-pinene and β-pinene by OH·and NO_3·. Specifically,
83 we report the hydrolysis lifetimes and the fraction of hydrolyzable $_p$ON formed in the systems examined in
84 this study. This comprehensive chamber study on the hydrolysis of $_p$ON produced from various oxidation
85 pathways of monoterpenes and peroxy radical (RO_2·) fates provides the fundamental data to better constrain
86 the role of hydrolysis in modulating $_p$ON concentrations and lifetimes in the atmosphere, their potential as
87 a NO_x loss pathway, and their impacts on overall nitrogen budget, O_3 and SOA formation.

2. Methods

2.1. Chamber experiment design and procedure

A series of chamber experiments were performed in the Georgia Tech Environmental Chamber facility (Boyd et al., 2015) housing two 12 m^3 Teflon reactors. Precursor volatile organic compounds (VOC) were α-pinene (99 %, Sigma-Aldrich) and β-pinene (99 %, Sigma-Aldrich) and the oxidation conditions of interest were OH· and NO_3· oxidation, which were represented as "daytime" and "nighttime" experiments, respectively. Specifically, four different systems of VOC and oxidation conditions were studied: α-pinene+OH·, β-pinene+OH·, α-pinene+NO_3·, and β-pinene+NO_3·. In order to infer the hydrolysis process, experiments were performed under low RH (i.e., ~5 %) or high RH (i.e., ~50-70 %) conditions and with effloresced or deliquesced seed particles for the same initial concentrations of precursor VOC and oxidant precursors. Temperature in the reactors was kept at room temperature (22-25ºC). Experimental conditions are summarized in Table 1.

Prior to every experiment, the reactor was flushed with zero air (AADCO, 747-14) for at least a day. A typical experiment began with the injection of seed aerosol into the reactor by atomizing dilute ammonium sulfate (AS; 0.015 M) or sulfuric acid + magnesium sulfate (SA+MS; 0.01 + 0.005 M) aqueous solution. The seed aerosol was either directly atomized into the reactor or passed through a dryer before entering the reactor. The difference between efflorescence RH (~35 %) and deliquescence RH (~80 %) for AS aerosol is fairly large (Seinfeld and Pandis, 2016). Taking advantage of this property, it is possible to vary the amount of water in aerosol under the same RH in the reactor. Initial seed number and volume concentrations upon atomization for 20 min were approximately 2×10^4 cm^{-3} and 2×10^{10} nm^3 cm^{-3}, respectively. A known amount of precursor VOC in the liquid form was transferred into a glass bulb, which was then evaporated and carried into the reactor by flowing zero air at 5 L min^{-1} through the bulb. Although the measurement of the precursor VOC concentration was not available for all experiments, the target and measured concentrations in the experiments when the measurements were available were consistent.

For "daytime" experiments, an oxidant precursor (i.e., H_2O_2) was introduced to the reactor in the same manner as VOC except that the glass bulb was gently heated by a heat gun to help evaporate faster. During the injection of H_2O_2, a desired amount of NO was introduced into the reactor from a cylinder containing 500 ppm NO (Matheson). For Exp. 3-5, 5 ppm NO at 5 L min^{-1} was continuously injected to the reactor until the SOA growth ceased. For Exp. 1, 2, 6, and 7, 15 ppm NO at 5 L min^{-1} was injected for 5-20 min several times until the SOA growth ceased. The NO concentration was usually on the order of tens of ppb and always remained above a few ppb, making the bimolecular reaction with NO a favorable $RO_2\cdot$ reaction pathway. The experiment was initiated by turning on the irradiation of UV light approximately 20 min after the end of the last injection to ensure that particles and vapors were mixed well inside the reactor.

The procedure for "nighttime" experiments was the same until the end of the precursor VOC injection. An oxidant precursor (i.e., N_2O_5) was pre-made in a flow tube by simultaneously injecting 500 ppm NO_2 (Matheson) at 0.4 L min^{-1} and ~250 ppm O_3 (Jelight 610) at 0.5 L min^{-1}. A simple kinetic box model was used to adjust the concentration of O_3 and flow rates of both NO_2 and O_3 to maximize the production of N_2O_5 and minimize the concentration of O_3, such that the VOC was dominantly oxidized by $NO_3\cdot$. Once N_2O_5 entered the reactor, it thermally decomposed to generate NO_2 and $NO_3\cdot$. VOC was usually depleted within the first 15 min of the experiment. For Exp. 8 and 14, the injection order of precursor VOC and oxidant precursor was switched such that the injection of VOC marked the beginning of the experiment. For Exp. 12 and 13, 25 ppm formaldehyde was added to the reactor to enhance the branching ratio of $RO_2\cdot+HO_2\cdot$ (Schwantes et al., 2015; Boyd et al., 2015) by injecting an appropriate amount of formalin solution (37 % HCHO, Sigma-Aldrich) in the same manner as the injection of H_2O_2. We do not discuss the details of the effect of the injection order nor the effects of the $RO_2\cdot$ fate here as they had negligible impact on the results concerning hydrolysis.

2.2. Instrumentation and data analysis

A High Resolution Time-of-Flight Aerosol Mass Spectrometer (HR-ToF-AMS; Aerodyne Research Inc.) measured the concentrations of non-refractory organics (Org), sulfate (SO_4), nitrate (NO_3),

ammonium (NH_4), and chloride (Chl) (DeCarlo et al., 2006). The data were analyzed using PIKA v1.16I and the unity collection efficiency was applied to all datasets. For the majority of nitrate-containing aerosol regardless of the class (i.e., inorganic or organic), the nitrate moiety (i.e., $-NO_2$, $-ONO_2$, and $-O_2NO_2$) was known to be thermally fragmented into NO^+ and NO_2^+ and was measured as NO_3 (Farmer et al., 2010). As many past studies have demonstrated the feasibility to separate the contribution of inorganic ($NO_{3,Inorg}$) and organic nitrate ($NO_{3,Org}$) to the measured NO_3 based on the ratio of NO^+ and NO_2^+ (Fry et al., 2009; Farmer et al., 2010; Xu et al., 2015b; Kiendler-Scharr et al., 2016; Fry et al., 2018), we used Eq. (1) presented in Farmer et al (2010) to obtain $NO_{3,Org}$. R_{AN} (i.e., NO^+/NO_2^+ from ammonium nitrate) was obtained from the routine ionization efficiency calibration of HR-ToF-AMS using 300 nm ammonium nitrate particles. The drawback of this method is that R_{ON} (i.e., NO^+/NO_2^+ from organic nitrate aerosol) could vary depending on the chemical composition (Xu et al., 2015b). In addition, a non-negligible contribution of ammonium nitrate could be expected in experiments with deliquesced seed aerosol owing to high solubility of HNO_3. Thus, we obtained the R_{ON} measured in low RH experiments for each system of VOC and oxidation condition. In order to account for changes in R_{AN} over time, R_{ON} was scaled accordingly assuming that the ratio of R_{ON} to R_{AN} in the same system was constant (Fry et al., 2013). R_{AN}, R_{ON}, and R_{ON}/R_{AN} values obtained in this study were consistent with previously reported values (Fry et al., 2009; Bruns et al., 2010; Boyd et al., 2015; Nah et al., 2016) and are summarized in Table S1.

A Filter Inlet for Gases and AEROsols (FIGAERO) (Lopez-Hilfiker et al., 2014) coupled to a High Resolution Time-of-Flight Iodide Chemical Ionization Mass Spectrometer (HR-ToF-I-CIMS; Aerodyne Research Inc.) detected a suite of gaseous and particulate oxidized organic species as well as selected inorganic species (Bertram et al., 2011; Lee et al., 2014). The operation of FIGAERO-HR-ToF-I-CIMS was detailed in the previous studies (Nah et al., 2016; Sanchez et al., 2016). Reagent ions were generated by flowing a mixture of CH_3I and dry ultra high purity (UHP) N_2 (Airgas) through a polonium-210 source (NRD; Model P-2021). The instrument measured gaseous compounds by sampling air from the reactor at ~1.7 L min^{-1} while collecting particles onto a Teflon filter. Upon completion of the collection period, collected particles were desorbed by temperature-programmed dry UHP N_2 flow and subsequently analyzed

by HR-ToF-I-CIMS. Sensitivity could decrease if the amount of reagent ions were significantly depleted and/or if the secondary chemistry in the ion-molecule reaction (IMR) chamber occurred at a significant degree (Lee et al., 2014). To avoid changes in sensitivity among experiments, gas-phase sampling flow was diluted with zero air immediately before the inlet such that the evaporation of aerosol was minimal. The amount of aerosol collected on the filter was also adjusted by varying the sampling rate from 1 to 6 L min^{-1} depending on the aerosol mass concentrations inside the reactor. Overall, the fraction of reagent ions to the total ions was kept above 80 %. In addition, iodide ion chemistry has been known to be affected by the water vapor pressure inside the IMR owing to the difference in thermodynamics between I^- and IH_2O^- to analyte compounds (Lee et al., 2014). In order to minimize changes in the water vapor pressure inside the IMR, a small continuous flow of humidified UHP N_2 (30-50 ccm) through a bubbler at a reduced pressure was continuously added to the IMR directly. Therefore, while the instrument was not calibrated to report the concentration of detected species, it was possible to quantitatively compare measured signal of each ion among experiments because the instrument was operated under configurations that prevented undesired changes in sensitivity. The data were analyzed using Tofware v2.5.11 and all the masses presented in this study were I^- adducts.

A Scanning Mobility Particle Sizer (SMPS) that consisted of a Differential Mobility Analyzer (TSI 3040) and a Condensation Particle Counter (TSI 3775) was operated under the low flow mode with the sheath flow of 2 L min^{-1} to detect particles up to 1 μm in electrical mobility size. A Cavity Attenuated Phase Shift spectroscopy (CAPS; Aerodyne Research Inc.) (Kebabian et al., 2005), an ultra-sensitivity NO_x analyzer (Teledyne M200EU), and an UV absorption O_3 analyzer (Teledyne T400) measured NO_2, NO_x, and O_3, respectively. In selected experiments, a Gas Chromatograph coupled to Flame Ionization Detector (GC-FID; Agilent) was used to make sure that a desired amount of a precursor VOC was injected. Except CAPS, NO_x analyzer, and O_3 analyzer, all instruments had their own dedicated sampling line.

3. Results and discussion

3.1. Chemical composition of secondary organic aerosol

Shown in Fig. 1 are the mass spectra of particle-phase species obtained from FIGAERO-HR-ToF-I-CIMS at peak SOA growth. Many of the major species detected in this study are previously reported using the same or different technique (Eddingsaas et al., 2012; Claflin and Ziemann, 2018; Boyd et al., 2015; Nah et al., 2016; Lee et al., 2016; Romonosky et al., 2017). Concerning the chemical composition of SOA from each system, a more distinct difference is observed between different oxidation conditions (i.e., OH· vs. NO_3· oxidation) than between different precursor VOC (i.e., α-pinene vs. β-pinene). This is expected as α-pinene and β-pinene have the same chemical formula and very similar structures while the oxidation condition is distinctively different (Kroll and Seinfeld, 2008; Ziemann and Atkinson, 2012).

For "daytime" experiments where OH· are the dominant oxidants, the contribution of ON (i.e., $C_xH_yN_{1,2}O_z$) and non-nitrated organics (i.e., $C_xH_yO_z$) are comparable and their contributions are well spread out over a wide range of masses. A large contribution of $C_xH_yO_z$ is expected because the formation of ON is a minor pathway in RO_2·+NO (Perring et al., 2013). In Eddingsaas et al. (2012), the major compounds reported in the α-pinene+OH· system include $C_8H_{12}O_{4\text{-}6}$ and $C_{10}H_{16}O_{4,6}$, which are also detected in our study. A suite of C_{10} ON from the chamber experiment of the α-pinene+OH· system are reported in Lee et al. (2016) with the chemical formula of $C_{10}H_{15,17,19}NO_{4\text{-}9}$. All of these masses are detected in this study, though we observe a considerable contribution of $C_{<10}$ ON (i.e., $C_7H_{9,11}NO_6$ and $C_9H_{13,15,17}NO_6$) as well as a small fraction of C_{10} dinitrate (i.e., $C_{10}H_{14,16}N_2O_{9,10}$) that has been rarely reported (Fig. 1a). This significant contribution from species containing $C_{<10}$ indicates the large contribution of fragmentation process that is a preferred pathway in high NO conditions (Kroll and Seinfeld, 2008; Ziemann and Atkinson, 2012; Perring et al., 2013). It is possible that these species with $C_{<10}$ are thermally decomposed products during the thermal desorption process (Stark et al., 2017). However, it is unlikely that thermal decomposition plays a significant role for the SOA generated via OH· oxidation of monoterpenes because the desorption temperature for these compounds (i.e., peaking at ~50-70 ºC) is much lower than the temperature at which decarboxylization or dehydration reactions (>120 ºC) are expected to occur (Stark et al., 2017). SOA chemical composition of the β-pinene+OH· system is similar to that of the α-pinene+OH· system but with a larger contribution of $C_xH_yO_z$.

Another interesting observation in the α-/β-pinene+OH· systems is that a selected class of compounds (i.e., $C_{10}H_{13,15,17}NO_{5\text{-}8}$) with the same H/C exhibit the same time evolutions regardless of the number of oxygen (Fig. S1). This observation is consistent with the autoxidation mechanism, in which highly oxidized molecules are formed in a short time scale (Ehn et al., 2014; Crounse et al., 2013; Jokinen et al., 2015). Based on FIGAERO-HR-ToF-I-CIMS data (Fig. S1), $C_{10}H_{17}NO_{\geq 6}$ peak at 75 min. This is comparable to the lifetime of α-pinene at 53 min in the same experiment, which is related to characteristic time of OH oxidation. This suggests that the aforementioned ON are likely formed via one OH oxidation reaction, which is consistent with the autoxidation scheme to generate $C_{10}H_{17}NO_{\geq 6}$ proposed in prior studies (Berndt et al., 2016; Xu et al., 2019; Pye et al., 2019). It is important to note that the concentration of NO in our experiments has been mostly kept on the order of tens of ppb over the course of the experiments by a continuous injection of dilute NO and, therefore, this result suggests that autoxidation is not a negligible pathway of RO_2· fate even at a moderately high NO level in laboratory experiments and in polluted ambient environments. Indeed, recent studies (Berndt et al., 2016; Xu et al., 2019; Pye et al., 2019) suggest that the autoxidation rate constant for the α-pinene+OH· system could be up to a few per second, which is comparable to the NO level of ~10 ppb, assuming a typical RO_2·+NO reaction rate constant of 1×10^{-11} cm^3 $molecule^{-1}$ s^{-1} (Orlando and Tyndall, 2012). The autoxidation rate constant as well as the role of NO in autoxidation based on this observation will be discussed in details in a forthcoming publication.

In contrast, the signals of $C_xH_yN_{1\text{-}2}O_z$ are dominant in the NO_3· oxidation condition, indicating that the production of ON is greatly favored over non-nitrated organics. This observation is consistent with a direct addition of a nitrate functional group to a double bond (Wayne et al., 1991; Ng et al., 2017), whereas the formation of ON in OH· oxidation condition is a minor channel of RO_2·+NO reaction (Perring et al., 2013). Although this is generally true for many monoterpenes, the organic nitrate yield in α-pinene+NO_3· has been known to be low (Fry et al., 2014) due to loss of a nitrate functional group followed by alkoxy radical bond scission (Kurten et al., 2017). Fry et al. (2014) observe no SOA formation in the same system, though another study has reported the formation of non-negligible SOA mass even at a relatively low initial concentration of α-pinene (Nah et al., 2016). Since the particle-phase compounds represent <10% of overall

α-pinene+NO_3· products by mass, it is not necessarily inconsistent to observe a higher abundance of ON than non-nitrated organics in the particle phase if low-volatility compounds mainly consist of ON.

Moreover, the contribution from species containing $C_{<10}$ is minimal in the NO_3· oxidation condition. Once NO_3· attacks a double bond in the initial oxidation reaction, the majority of the reaction products no longer contain any double bond. Unlike OH·, a hydrogen abstraction reaction by NO_3· is slower by orders of magnitude (Atkinson and Arey, 2003). Therefore, multi-generation oxidation is unlikely to occur within the timescale of experiments (Wayne et al., 1991; Ng et al., 2017). This means that once the precursor VOC undergoes functionalization upon the initial NO_3· oxidation, it is not likely to experience fragmentation during the experiment. Unlike "daytime" SOA, the distribution of masses is dominated by a few signature ions, such as $C_{10}H_{15}NO_{5,6}$ and $C_{20}H_{32}N_2O_{8\text{-}10}$ (Fig. 1c and 1d). In Boyd et al. (2015), Nah et al. (2016), and Lee et al. (2016), the major species reported in the α-/β-pinene+NO_3· systems are monomeric nitrate aerosol (i.e., $C_{10}H_{13,15,17,19}NO_{4\text{-}10}$), while in this study a substantial contribution of dimeric species (i.e., $C_{20}H_{32}N_2O_{8\text{-}11}$) is observed. The abundant presence of dimeric compounds has been previously observed in some studies on NO_3· oxidation of α-/β-pinene (Romonosky et al., 2017; Claflin and Ziemann, 2018) and particle-phase reactions to produce such dimers have been proposed by Claflin and Ziemann (2018). Many of the reported species in Claflin and Ziemann (2018) except the trimeric species (mass scan range not extended to trimeric species in our study) are observed in our study. One major difference between Claflin and Ziemann (2018) and this study is the substantial presence of monomeric nitrate aerosol (i.e., 30-60 % by signal) in this study. This difference may be attributed to the difference in the amount of available monomeric blocks to form dimer species. Assuming reversible dimerization process, the concentration of dimer species shall be proportional to the square of monomer concentration, such that the monomer to dimer ratio increases in a quadratic manner as the available monomer concentration decreases. Since the amount of SOA formed in Claflin and Ziemann (2018) is approximately two orders of magnitude higher than that in this study, the concentration of monomers in the particle-phase is higher, favoring a more efficient formation of dimeric species. Together, these results suggest that the contribution of dimeric

nitrate aerosol could vary greatly depending on the concentrations of monomeric blocks at the specific time and location.

Previous field studies have reported the mass spectra of ambient C_{10} $_{p}$ON obtained by FIGAERO-HR-ToF-I-CIMS in rural Alabama site during the Southern Oxidant and Aerosol Study (SOAS) (Lee et al., 2016) and in rural forest in Germany (Zhang et al., 2018). A comparison of the ambient mass spectra with those obtained in this study reveals that average ambient $_{p}$ON resembles "daytime" $_{p}$ON more than "nighttime" $_{p}$ON (Fig. S2). $_{p}$ON from "daytime" experiments has a distribution of masses centered around $C_{10}H_{13,15,17}NO_7$, which is consistent with the ambient measurement data. On the other hand, NO_3· oxidation does not seem to oxidize organic species enough that the distribution of masses is skewed towards a less-oxidized region (i.e., $C_{10}H_{13,15,17}NO_{5\text{-}6}$). However, it is difficult to draw a quantitative conclusion simply based on this comparison because O_3, another important oxidant at night, is not studied. Moreover, an average lifetime of aerosol could extend up to a week and thus ambient aerosol is continuously exposed to further oxidation while the experiments here are more applicable to freshly formed aerosol. In addition, the use of C_{10} $_{p}$ON alone may not be a good representative of monoterpene-derived $_{p}$ON as 42-74 % of $_{p}$ON in this study contains fewer or more than 10 carbon (Table S2). Nonetheless, the chemical composition of aerosol generated in this study is comparable to those in the atmosphere and, thus, the results shall be directly applicable to relevant ambient conditions.

3.2. Hydrolysis of particulate organic nitrate

3.2.1. Proxy used to evaluate hydrolysis process

Various proxies using HR-ToF-AMS data have been used to infer ON hydrolysis in previous studies. In Bean and Hildebrandt Ruiz (2016), NO_3 measured by an Aerosol Chemical Speciation Monitor (ACSM, practically similar to how AMS operates and measures aerosol species) (Ng et al., 2011) is normalized to SO_4 as a means to account for particle wall-loss and is fitted by an exponential function to estimate the ON hydrolysis rate. On the other hand, Boyd et al. (2015) normalize NO_3 measured by HR-ToF-AMS to Org and attribute the relative decay of NO_3/Org between humid (RH ~50 %) to dry (RH <5

294 %) conditions to hydrolysis. Other approaches include the SMPS-derived particle wall-loss correction of
295 NO_3 measured by HR-ToF-AMS followed by fitting its decay trend (Liu et al., 2012b) and the determination
296 of fraction of total (i.e., gas and particle) ON to the precursor VOC consumed as a function of RH using a
297 Fourier-Transform InfraRed spectroscopy (FTIR). Below, we systematically examine the use of different
298 proxies using HR-ToF-AMS data to infer hydrolysis and discuss how the corresponding results are
299 interpreted.

300 Figure 2 shows the time series of Org, NO_3, SO_4, and NH_4 measured by HR-TOF-AMS for α-
301 pinene+NO_3· system. There is a substantial difference in NO_3 for the same VOC system but under different
302 reactor RH and phase state of seed particles (Exp. 10 and 11), while Org and SO_4 concentrations are similar.
303 The spike in NO_3 in high RH wet seed experiment (Fig. 2b) is attributed to the uptake of N_2O_5 and/or
304 dissolution of HNO_3 into aqueous aerosol followed by neutralization with ammonia to produce ammonium
305 nitrate. This is consistent with the sharp increase in molar ratio of NH_4/SO_4 to higher than 2, which is the
306 theoretical value for AS particles. It is also possible that inorganic nitrate is generated via hydrolysis of
307 gaseous ON that is too volatile to condense but is soluble enough to dissolve in aqueous aerosol and, thus,
308 only appears in high RH experiments. Since we do not have a way to quantitatively differentiate the
309 contribution of the aforementioned sources, the focus of this study is on hydrolysis of $_pON$ that partitions
310 to the aerosol due to condensation rather than dissolution. However, further study is required to investigate
311 the hydrolysis of volatile yet soluble gaseous ON, and the approach must be different from the comparison
312 between low and high RH experiments to obtain meaningful results.

313 To evaluate the extent of $_pON$ hydrolysis, the contributions of inorganic nitrate ($NO_{3,Inorg}$) and
314 organic nitrate ($NO_{3,Org}$) to the measured NO_3 need to be calculated. Firstly, $NO_{3,Org}$ is estimated by
315 subtracting NO_3 associated with excess NH_4. Secondly, $NO_{3,Org}$ is derived from NO^+/NO_2^+ approach (Sect.
316 2.2.). Figure S3 shows the comparison of $NO_{3,Org}$ estimated by these two independent methods for the α-
317 pinene+NO_3· system. It is clear that $NO_{3,Org}$ from both methods are consistent and that there is a
318 considerable contribution of $NO_{3,Inorg}$ to NO_3 in the experiment. We note the contribution of $NO_{3,Inorg}$ to NO_3
319 can vary depending on experimental conditions with a range from to 28 to 90 % for all experiments in this

study. Nevertheless, these results demonstrate that for laboratory experiments with high RH and wet seeds, when using HR-ToF-AMS data to infer hydrolysis, it is important to separate the measured NO_3 into $NO_{3,Inorg}$ and $NO_{3,Org}$.

Once NO_3 is separated into $NO_{3,Inorg}$ and $NO_{3,Org}$, we evaluate whether the normalization of $NO_{3,Org}$ to SO_4 and Org provides a consistent decay trend. Photooxidation of α-pinene (Exp. 3-5) is used as a case system. As hydrolysis is a reaction in which liquid water is a reactant, it is expected that the rate of hydrolysis will change proportionally as a function of aerosol water content. Based on the hygroscopicity parameter for AS ($\kappa = 0.53$) (Petters and Kreidenweis, 2007) and for ambient LO-OOA ($\kappa = 0.08$) (Cerully et al., 2015) that has a substantial contribution from $_pON$ (Xu et al., 2015a), estimated aerosol water contents at peak SOA growth in Exp. 3-5 are approximately 0, 1, and 26 μg m^3, respectively. Figure S4 illustrates that AS seed particles are indeed effloresced in Exp. 4 (high RH, dry AS) but not in Exp. 5 (high RH, wet AS). These mass concentrations of aerosol water translate to 0, 6, and 36 mol L^{-1}, respectively, under the assumption that SOA is miscible with liquid water. It is speculated that SOA formed in Exp. 3-5 are miscible with water because (1) the measured O/C ratio in HR-ToF-AMS (Canagaratna et al., 2015) is close to 0.7, which is near the lower end but above the liquid-liquid phase separation condition (Song et al., 2012) and (2) there is evidence of aqueous-phase reactions which highly depend on the availability of aerosol water, as discussed in Sect. 3.3. Thus, the decay rate of $NO_{3,Org}$ normalized to SO_4 and/or Org between Exp. 4 and Exp. 5 shall differ by a factor of 6 based on the molar concentrations of aerosol water.

Figure 3a shows the mass ratio of $NO_{3,Org}/SO_4$ and the decay rate as a characteristic time in Exp. 3-5. The characteristic times of Exp. 4 and 5 (4.4 vs. 4.0 h) do not differ regardless of the molar concentrations of aerosol water, suggesting that the decreasing trend in $NO_{3,Org}/SO_4$ may not be due to changes in aerosol water content and $_pON$ hydrolysis, but arise from the difference in the reactor humidity alone. A comparison of $NO_{3,Org}/SO_4$ and $NO_{3,Org}$/Org also reveals that these two proxies capture a different range of decay mechanisms. Figure 3b shows the relative decay trend of $NO_{3,Org}/SO_4$ and $NO_{3,Org}$/Org between Exp. 4 (high RH) and Exp. 3 (low RH). If hydrolysis is a dominant decay mechanism of $_pON$, the trend of $NO_{3,Org}$/Org would be identical to that of $NO_{3,Org}/SO_4$. This is because the organic moiety of hydrolysis product is

generally considered to have a substituted alcohol group (Boschan et al., 1955) and to have a relatively similar vapor pressure and shall remain in the particle phase (Pankow and Asher, 2008). Similar to this is the formation of organic sulfate from hydrolysis of $_{p}$ON (Liggio and Li, 2006, 2008; Surratt et al., 2008), which has sufficiently low volatility to remain in the particle phase as with alcohol substituted products. However, the measured decay trend of the two proxies is greatly different. It is possible that some organic moiety of hydrolysis product could be significantly more volatile and repartition back to the gas phase (Rindelaub et al., 2016; Bean and Hildebrandt Ruiz, 2016) and, thus, both organics and HNO_3 formed from hydrolysis evaporate. In this case, not only $NO_{3,Org}$ but also some fraction of Org would decrease because Org measured by HR-ToF-AMS includes the contribution from the organic part of $_{p}$ON. This will lead to the relatively smaller decrease in $NO_{3,Org}$/Org compared to $NO_{3,Org}/SO_4$. We can reconstruct the decay rate of $NO_{3,Org}$/Org assuming 1) the decay rate of $NO_{3,Org}/SO_4$ is solely due to hydrolysis of $_{p}$ON and 2) the maximum contribution of $_{p}$ON to OA is 35 % (see Fig. 4 and discussions below). The reconstructed decay rate of $NO_{3,Org}$/Org is shown in Fig. 3b. As observed in the figure, the decay rate of the reconstructed $NO_{3,Org}$/Org is much larger than the measured $NO_{3,Org}$/Org. This suggests that hydrolysis is not the only loss process reflected in the decreasing trend of $NO_{3,Org}/SO_4$, while $NO_{3,Org}$/Org is likely a better proxy that isolates hydrolysis from other loss processes. The likely important loss process manifested in $NO_{3,Org}/SO_4$ is the loss of organic vapors to the walls of the reactor (Matsunaga and Ziemann, 2010; Krechmer et al., 2016; Huang et al., 2018; Loza et al., 2010; Mcvay et al., 2014; Zhang et al., 2015; Zhang et al., 2014; La et al., 2016). For example, Huang et al. (2018) observe that the decay of isoprene hydroxy nitrate depends on the reactor humidity. While SO_4 is practically non-volatile in the experimental condition of this study, both ON and non-nitrated organics could have some fractions of semi-volatile species whose vapors are subject to wall loss. Assuming a uniform loss rate of ON and non-nitrated organic vapors to the reactor walls, the effect of vapor wall loss could be effectively cancelled out in $NO_{3,Org}$/Org, but not in $NO_{3,Org}/SO_4$. This assumption is likely reasonable because the vapor wall loss rate is a function of saturation mass concentration (Zhang et al., 2015) and the average saturation mass concentrations of bulk ON and non-

nitrated organic aerosol are similar based on the thermal desorption profiles in FIGAERO-HR-ToF-I-CIMS (Fig. S5). Therefore, $NO_{3,Org}$/Org is a better proxy to infer hydrolysis of $_pON$ than others.

3.2.2. Hydrolysis lifetime of particulate organic nitrate

In order for the data to be easily comparable with those reported in models or using other techniques, the use of general terms instead of the AMS specific terms (i.e., $NO_{3,Org}$ and Org) can be convenient. We define $_pON$ as the total mass concentration of particulate organic nitrate (includes organics part and nitrate part of the ON compounds) and OA as the total mass concentration of organic aerosol (includes nitrate and non-nitrated organics). The inclusion of nitrate mass concentration in OA is important as the contribution of nitrate functional groups to the total organic aerosol mass concentration is large. The conversion method from $NO_{3,Org}$/Org into $_pON$/OA is illustrated in Eq. (1).

$$\frac{_pON}{OA} = \left(\frac{NO_{3,Org}}{Org + NO_{3,Org}}\right) \times \left(\frac{MW_{_pON}}{MW_{NO_3}}\right) = \left(\frac{\frac{NO_{3,Org}}{Org}}{1 + \frac{NO_{3,Org}}{Org}}\right) \times \left(\frac{MW_{_pON}}{MW_{NO_3}}\right) \quad (1)$$

MW_{pON} represents the average molecular weight of $_pON$ per nitrate functional group estimated from FIGAERO-HR-ToF-I-CIMS data assuming a uniform sensitivity among detected species, and MW_{NO3} indicates the molecular weight of nitrate (i.e., 62 g mol^{-1}). Since MW_{pON} does not significantly vary during the course of experiments (i.e., relative standard deviation of <1.2 %), the average value is applied to each experiment. The variability of MW_{pON} among different systems is also found to be small, ranging from 229 to 238 g mol^{-1} and, thus, an average MW_{pON} is used for experiments where FIGAERO-HR-ToF-I-CIMS data are not available. Figure 4 shows the time-series data of $_pON$/OA for all the systems investigated in this study.

For "nighttime" experiments, the relative ratio of $C_xH_yN_{1\text{-}2}O_z$ and $C_xH_yO_z$ obtained from FIGAERO-HR-ToF-I-CIMS data in Fig. 1 does not appear to match well with $_pON$/OA from HR-ToF-AMS data. For example, the signals are dominated by $C_xH_yN_{1\text{-}2}O_z$ in the β-pinene+NO_3· system, as shown in Fig. 1d, while $_pON$/OA is at most 0.5, as shown in Fig. 4d. The discrepancy would be attributed to the

overestimation of Org (in particular, C_xH_y family) in HR-ToF-AMS and/or underestimation of $C_xH_yO_z$ in FIGAERO-HR-ToF-I-CIMS. Relative ionization efficiency (RIE) of less-oxidized organic species in HR-ToF-AMS is experimentally measured to be higher at least by a factor of 2 (Xu et al., 2018b). As previously reported (Boyd et al., 2015), the HR-ToF-AMS mass spectrum of SOA formed from β-pinene+NO_3· contains significant amounts of C_xH_y fragments, indicating the less-oxidized nature of SOA from β-pinene+NO_3·. For example, if the true RIE of Org by β-pinene+NO_3· SOA were to be a factor of 2 higher than the default RIE of Org (i.e., 1.4), the reported concentration of Org would have been overestimated by a factor of 2, such that actual $_p$ON/OA would have been higher than reported in Fig. 4d. On the other hand, an iodide reagent ion is not quite selective to detect less oxidized species, which could overestimate the contribution of $_p$ON to OA (Aljawhary et al., 2013). Nonetheless, this discrepancy between HR-ToF-AMS and FIGAERO-HR-ToF-I-CIMS data, however, should not affect the results regarding the hydrolysis lifetime and hydrolyzable fraction of $_p$ON presented later.

As illustrated in Fig. 4, the time series of $_p$ON/OA stabilizes fairly quickly in most of the experiments, regardless of RH and/or the phase state of seed aerosol, supporting the appropriateness of the reconstructive approach shown in Fig. 3b. This suggests that the timescale of $_p$ON hydrolysis in the systems studied is significantly shorter or longer than the timescale of our experiments. It is also evident from Fig. 4 that $_p$ON/OA in high RH experiments are always lower than that in low RH experiments. These two observations imply that the rate of $_p$ON hydrolysis may be fast enough that the decay trend of $_p$ON compared to OA is not visibly manifested, though a clear difference of $_p$ON/OA between low and high RH experiments is exhibited as a result of fast hydrolysis. Since no sudden, drastic change in $_p$ON/OA is observed except for a few initial data points, we conclude that the hydrolysis lifetime of hydrolyzable $_p$ON for α-/β-pinene derived ON shall be no more than 30 min (i.e., 3 data points in Fig. 4). Particle acidity is found to enhance hydrolysis rate of α-pinene hydroxy nitrate (Rindelaub et al., 2016), though no clear difference is observed here between experiments with AS and SA+MS seed particles (i.e., Exp. 5 and 2). It is worth noting that aqueous AS particles are not neutral but slightly acidic due to partitioning of ammonium to the gas phase once the particles enter the chamber (Gao et al., 2004). In Gao et al. (2004), the reported

pH of aqueous AS particles is 4.6 and we expect a similar pH in our study. In Rindelaub et al. (2016), the reported hydrolysis lifetime is short at 1.3 h at pH of 4.0. On the other hand, previous studies have shown that isoprene-derived hydroxy nitrates do not require low pH to undergo fast hydrolysis (Darer et al., 2011; Hu et al., 2011). Thus, $_{p}$ON formed from OH· and NO_3· oxidation of α-pinene and β-pinene may not require a low pH to undergo hydrolysis at a rate comparable to the timescale of chamber experiments.

Comparing with the results from past chamber studies reporting a $_{p}$ON hydrolysis lifetime of 3 to 6 h (Liu et al., 2012b; Bean and Hildebrandt Ruiz, 2016; Boyd et al., 2015), our estimated hydrolysis lifetime is substantially shorter, but is consistent with the range (i.e., 1 min to 8.8 h) reported in studies using the bulk solution method (Darer et al., 2011; Hu et al., 2011; Jacobs et al., 2014; Rindelaub et al., 2016) (Fig. 5). In Liu et al. (2012) and Bean and Hildebrandt Ruiz (2016), the hydrolysis lifetime is derived from the decay rate of NO_3 corrected for the particle wall loss or normalized to SO_4. As demonstrated in Sect. 3.2.1., this NO_3/SO_4 decay rate is likely affected by other loss processes, such as vapor wall loss, and, thus, is not a good proxy to estimate the hydrolysis lifetime. The apparent discrepancy does not stem from the contradiction in the obtained data itself but rather in the data interpretation. Indeed, the lifetime estimated based on the decay of $NO_{3,Org}/SO_4$ in our study is 4 h (Fig. 3a) that is consistent with 6 and 3 h reported in Liu et al. (2012) and Bean and Hildebrandt Ruiz (2016). On the other hand, in Boyd et al. (2015) the hydrolysis lifetime is estimated based on the decay rate of NO_3/Org. The discrepancy in the reported hydrolysis lifetime here could be attributed to the fact that NO_3 is not separated into $NO_{3,Org}$ and $NO_{3,Inorg}$. Figure S6 shows our data analyzed in the same manner as Boyd et al. (2015). The lifetime calculated based on the decay is 2.2 h, which is close to the reported 3-4.5 h (Boyd et al., 2015). The reduction of NO_3/Org in Fig. S6 (~30 %) is greater than in Boyd et al. (2015) (10 %), which could be because (1) the amount of N_2O_5, a source of inorganic nitrate, used in our study is slightly larger and (2) RH in our study is higher by 10-20 %, which may have allowed greater uptake of N_2O_5 to produce inorganic nitrate due to changes in aerosol viscosity (Grzinic et al., 2015).

In previous bulk solution studies where the concentration of interested organic nitrate (in particular hydroxy nitrate) in aqueous solution rather than in aerosol water is monitored over time, it is unlikely that

446 the data interpretation is affected by other loss processes present in chamber experiments, such as vapor
447 wall-loss. It is also common to monitor the organic moiety of hydrolysis product (Darer et al., 2011), while
448 it is extremely difficult in chamber experiments where hundreds of organic species are present at the same
449 time, leading to the difficulty in accurately measuring the hydrolysis lifetime in chamber experiments.
450 Based on the comprehensive analysis we demonstrate above on evaluating $_{p}$ON hydrolysis in chamber
451 experiments, we recommend the use of the hydrolysis lifetime reported in this study, which is no more than
452 30 min, for $_{p}$ON formed from α-pinene and β-pinene.
453
454 3.2.3. Hydrolyzable fraction of particulate organic nitrate
455 The fraction of hydrolyzable $_{p}$ON (F_H) can be directly estimated from the difference in $_{p}$ON/OA
456 between low and high RH experiments shown in Fig. 4. Although we show that hydrolysis is substantially
457 faster than the timescale of chamber experiments in our study, there still appears a clear difference in
458 $_{p}$ON/OA between high RH experiments but with a different phase state of seed aerosol (i.e., Exp. 4 and 5).
459 The difference mass spectra among Exp. 3-5 obtained from FIGAERO-HR-ToF-I-CIMS reveal that the
460 difference in $_{p}$ON/OA between Exp. 4 and 5 does not arise from the reduction in $_{p}$ON but from the increase
461 in non-nitrated organics (Fig. 6). The reason for this OA increase with the abundant presence of aerosol
462 water is speculated to be uptake and other aqueous-phase reactions than hydrolysis and is briefly discussed
463 in Sect. 3.3. Thus, the absolute difference in $_{p}$ON/OA between low RH, dry seed and high RH, dry seed
464 experiments best indicates F_H. Depending on the fate of the organic moiety of the hydrolysis product (i.e.,
465 stay in the particle phase or repartition back to the gas phase), F_H varies. Since we are unable to determine
466 the fate of hydrolysis product, an upper and lower limit of F_H are reported as a range of F_H. For the α-
467 pinene+OH· system, 23-32 % of $_{p}$ON formed undergoes hydrolysis within the timescale of the experiments.
468 For the other systems with no experiment under high RH with dry seed aerosol, the same level of additional
469 contribution from non-nitrated organics encountered in α-pinene+OH· system is assumed and F_H is scaled
470 accordingly. For the β-pinene+OH·, α-pinene+NO_3·, and β-pinene+NO_3· systems, 27-34, 9-17, and 9-15 %

of $_{p}$ON are found hydrolyzable within the timescale of the experiments. Table 2 summarizes the hydrolysis lifetime and F_H in the systems explored in this study.

F_H has been only reported in a few studies (Liu et al., 2012b; Boyd et al., 2015; Zare et al., 2018). The determination of F_H is essential because the assumption that all $_{p}$ON hydrolyzes biases the relative importance of hydrolysis among the loss mechanisms of $_{p}$ON and NO_x. Boyd et al. (2015) report that F_H of $_{p}$ON formed via β-pinene+NO_3· is ~10 %, which is in a good agreement with our range of 9-15 %. From a perspective of predicted molecular structures of $_{p}$ON, <5 % of $_{p}$ON from β-pinene+NO_3· are tertiary (Claflin and Ziemann, 2018) that is expected to undergo hydrolysis in minutes (Darer et al., 2011; Hu et al., 2011). In our study, a considerable contribution of monomeric (C_{10}) $_{p}$ON is observed (Fig. 1d), while dimeric (C_{20}) $_{p}$ON is dominant in Claflin and Ziemann (2018). This may indicate that monomeric $_{p}$ON is more susceptible to hydrolysis such that F_H in this study is slightly higher than expected based on the proposed molecular structures of $_{p}$ON in Claflin and Ziemann (2018).

F_H for α-/β-pinene+OH· systems are higher than those from α-/β-pinene+NO_3· systems. This trend is consistent with the understanding that $_{p}$ON via OH· oxidation have a larger fraction of tertiary nitrate groups, which are significantly more susceptible to hydrolysis (Darer et al., 2011; Hu et al., 2011) than those formed via NO_3· oxidation (Ng et al., 2017). Although the relative trend of F_H between α-/β-pinene+OH· and α-/β-pinene+NO_3· systems is consistent, the magnitude of F_H in the α-/β-pinene+OH· system appears to be smaller than expected based on the tertiary nitrate fraction estimated via the explicit gas-phase chemical mechanism (Browne et al., 2013; Zare et al., 2018). In previous studies, F_H are estimated to be 62 and 92 % for α-/β-pinene+OH· systems, respectively. However, our results indicate F_H is 23-32 and 27-34 % for the same systems (Fig. 5). The chemical mechanism used in Browne et al. (2013) and Zare et al. (2018) are based on the Master Chemical Mechanism (MCM) that is well known in the degradation chemistry of VOC in the gas phase (Jenkin et al., 1997; Saunders et al., 2003). However, the same mechanism performs poorly in regards to the chemical composition of SOA (Faxon et al., 2018) as well as the prediction of SOA formation (Ruggeri et al., 2016; Boyd et al., 2017) when equipped with gas-particle partitioning modules based on the absorptive gas-particle partitioning theory (Pankow, 1994). It is,

497 therefore, reasonable to argue that the chemical composition of $_{p}$ON could greatly differ from that of total
498 ON predicted by the MCM. Thus, F_H reported in this study provides the fundamental experimental
499 constraints on $_{p}$ON hydrolysis, that can be used in regional and global models for elucidating potential
500 impacts of ON on nitrogen budget and formation of ozone and aerosol.
501
502 3.3 Signature of other aqueous-phase reactions than hydrolysis
503 As briefly discussed in the above section, the presence of elevated level of aerosol water seems to
504 have enhanced the contribution of small (i.e., $C_{<9}$) but more-oxidized organic species to SOA. As shown in
505 Fig. 5c, the enhancement is observed for a variety of non-nitrated organic aerosol including $C_4H_{6,8}O_3$,
506 $C_4H_4O_4$, $C_5H_6O_5$, $C_7H_{8,10}O_4$, and $C_8H_{8,10}O_{4,5}$, while $_{p}$ON overall neither increase nor decrease. $C_5H_6O_5$ has
507 been reported as a product of the aqueous-phase reaction of α-pinene derived compounds (Aljawhary et al.,
508 2016). Other compounds, such as $C_4H_4O_4$, $C_7H_{8,10}O_4$, and $C_8H_{10}O_5$, also appear to result from the aqueous
509 processing because compounds with similar chemical formulae but with slightly higher degrees of oxidation
510 (i.e., $C_4H_4O_5$, $C_7H_{10}O_5$, and $C_8H_{12}O_6$) are reported in Aljwhary et al. (2016). The reason for this less
511 oxidized nature of SOA in this study may be attributed to our experiments being performed in moderately
512 high NO conditions that promotes a higher contribution of a carbonyl group than a hydroperoxyl group,
513 which is preferred in low NO conditions. In Aljwhary et al. (2016), the starting compound is a product in
514 low NO conditions (pinonic acid, $C_{10}H_{16}O_3$). Thus, it is reasonable that products of the aqueous processing
515 in this study are slightly less oxidized than observed in Aljwhary et al. (2016).
516 The enhancement of non-nitrated organic aerosol in FIGAERO-HR-ToF-I-CIMS may be due to
517 aqueous processing of species in the particles in the presence of aerosol water. This can come from further
518 reactions of semi/low-volatile species in the particle phase, or reactive uptake of volatile (but highly water-
519 soluble) species into the aerosol followed by subsequent aqueous-phase reactions to form low-volatility
520 products (Ervens et al., 2011). A comparison of the average thermogram at peak SOA growth among Exp.
521 3-5 indicates a higher contribution of low-volatility compounds in Exp. 5 than in Exp, 3 and 4, as illustrated
522 by the bimodal peaks (Fig. S7). Given the same degree of gas-phase oxidation expected among Exp. 3-5,

these results show that that aqueous chemistry in wet aerosol contributes to the further formation of low-volatility compounds. Overall, the highest average degree of oxidation (O/C = 0.77) is observed in high RH wet aerosol experiment (Expt. 5). The effect of particle water on monoterpene SOA formation warrants further studies.

3.4 Atmospheric implications

There is emerging evidence that monoterpene SOA greatly contribute to atmospheric aerosol in the Southeastern U.S. (Zhang et al., 2018; Xu et al., 2018a). ON is no exception; a substantial fraction of $_{p}$ON is considered to be from monoterpenes (Lee et al., 2016; Huang et al., 2019; Xu et al., 2015a). While C_{10} $_{p}$ON measured in FIGAERO-HR-ToF-I-CIMS is a good tracer of monoterpene derived $_{p}$ON, we show that a fair amount of α-/β-pinene $_{p}$ON is found as $C_{<10}$ or C_{20} depending on the oxidation condition. This implies that the contribution of monoterpene derived $_{p}$ON could be substantially underestimated when only considering C_{10} $_{p}$ON. Fraction of $_{p}$ON with different number of carbon reported in this study (Table S2) is a useful parameter to quantitatively determine the contribution of monoterpenes derived $_{p}$ON to total $_{p}$ON.

Many previous modeling studies using ambient measurement data as constraints report that the lifetime of $_{p}$ON is likely several hours (Pye et al., 2015; Fisher et al., 2016; Lee et al., 2016; Zare et al., 2018). Hydrolysis of $_{p}$ON is used as a dominant loss process with the lifetime of several hours to improve the concentration of modeled OA (Pye et al., 2015) and to improve the concentrations of gaseous and particulate ON (Fisher et al., 2016). If the ambient $_{p}$ON concentration is indeed governed by a loss process with a few hours of lifetime, our results imply that the particle-phase hydrolysis may not be the only dominant loss process because the hydrolysis lifetime reported in this study is significantly shorter. Other potential but less-studied loss mechanisms of ON and $_{p}$ON include deposition (Nguyen et al., 2015), photolysis (Muller et al., 2014), and aqueous photooxidation (Romonosky et al., 2017; Nah et al., 2016). For instance, enhanced photolysis rate is observed for carbonyl nitrate derived from isoprene (Muller et al., 2014), while no similar study is available for monoterpene derived ON in literature. Also, it has been demonstrated that different monoterpene $_{p}$ON can have drastically different photochemical fates (Nah et

549 al., 2016). Taken together, results from this study highlight the importance to investigate other potential
550 loss processes of monoterpene derived $_{p}$ON.

551 Aside from the hydrolysis lifetime, many modeling studies assume F_H as unity (Pye et al., 2015;
552 Fisher et al., 2016; Lee et al., 2016). Even when F_H is considered, the value of F_H used in other studies is
553 still substantially higher than estimated in this study (Browne et al., 2013; Zare et al., 2018). The use of
554 higher F_H would result in overestimating the contribution of hydrolysis as a loss process of $_{p}$ON and NO_x.
555 While hydrolysis is considered as a permanent sink of NO_x, many other loss processes, such as further OH·
556 oxidation and photolysis, are considered as a temporary reservoir of NO_x. If the relative importance of $_{p}$ON
557 fates in models was not accurate, the role of ON in NO_x cycling and the formation potential of ozone could
558 have been inaccurately interpreted. Therefore, results from this study regarding the hydrolysis lifetime and
559 F_H serve as experimentally constrained parameters for chemical transport models to accurately evaluate the
560 role of ON in regards to nitrogen budget and the formation of ozone and fine aerosol.
561

562 **Author contribution**

563 M.T. designed and performed the research and analyzed the data with substantial inputs from N.L.N. M.T.
564 and N.L.N. wrote the manuscript.
565

566 **Acknowledgements**

567 The authors would like to acknowledge financial support by National Science Foundation (NSF) CAREER
568 AGS-1555034 and by National Oceanic and Atmospheric Administration (NOAA) NA18OAR4310112.
569 The FIGAERO-HR-ToF-CIMS has been purchased through NSF Major Research Instrumentation (MRI)
570 Grant 1428738.
571

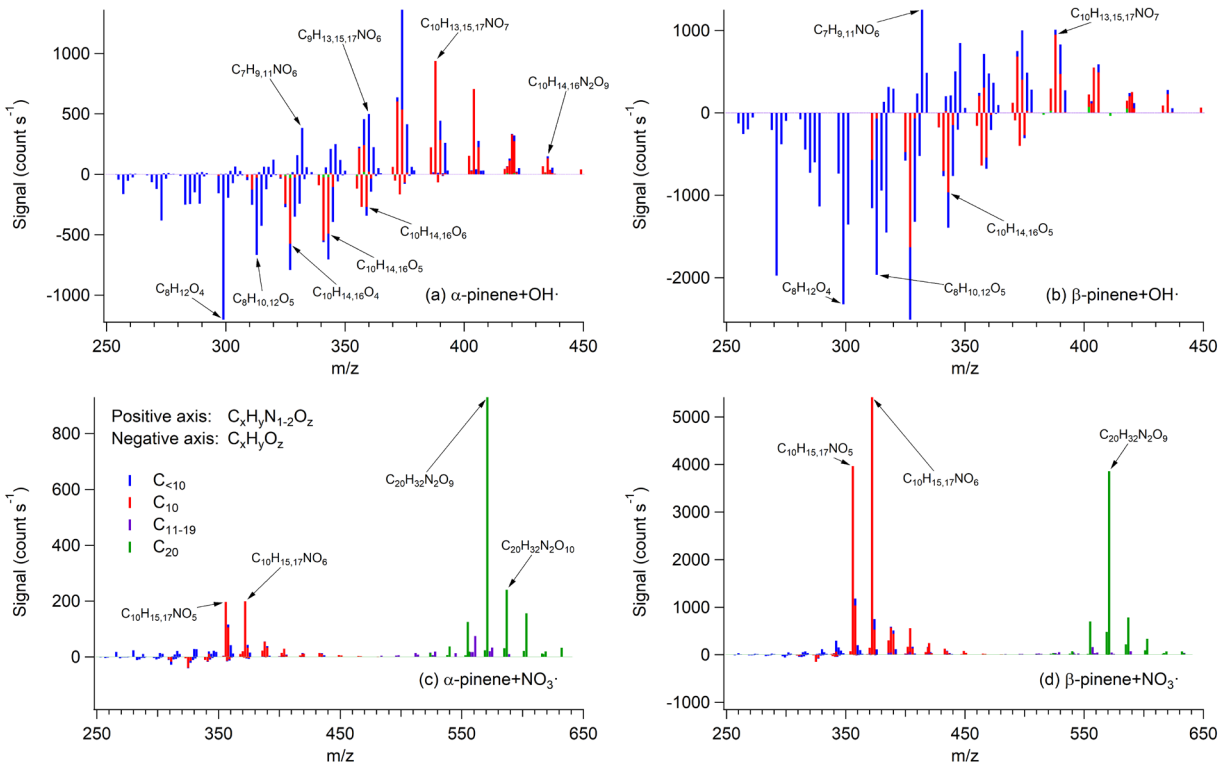

572

573 Figure 1. FIGAERO-HR-ToF-I-CIMS mass spectra of SOA in (a) α-pinene+OH· from Exp. 3, (b) β-
574 pinene+OH· from Exp. 6, (c) α-pinene+NO_3· from Exp. 10, and (d) β-pinene+NO_3· from Exp. 14. Top
575 portion of each panel represents $C_xH_yN_{1\text{-}2}O_z$, whereas bottom represents $C_xH_yO_z$. Bars are colored by the
576 number of carbon as noted in the legend. Prominent masses are labeled with the corresponding chemical
577 formulae without an iodide ion.

578

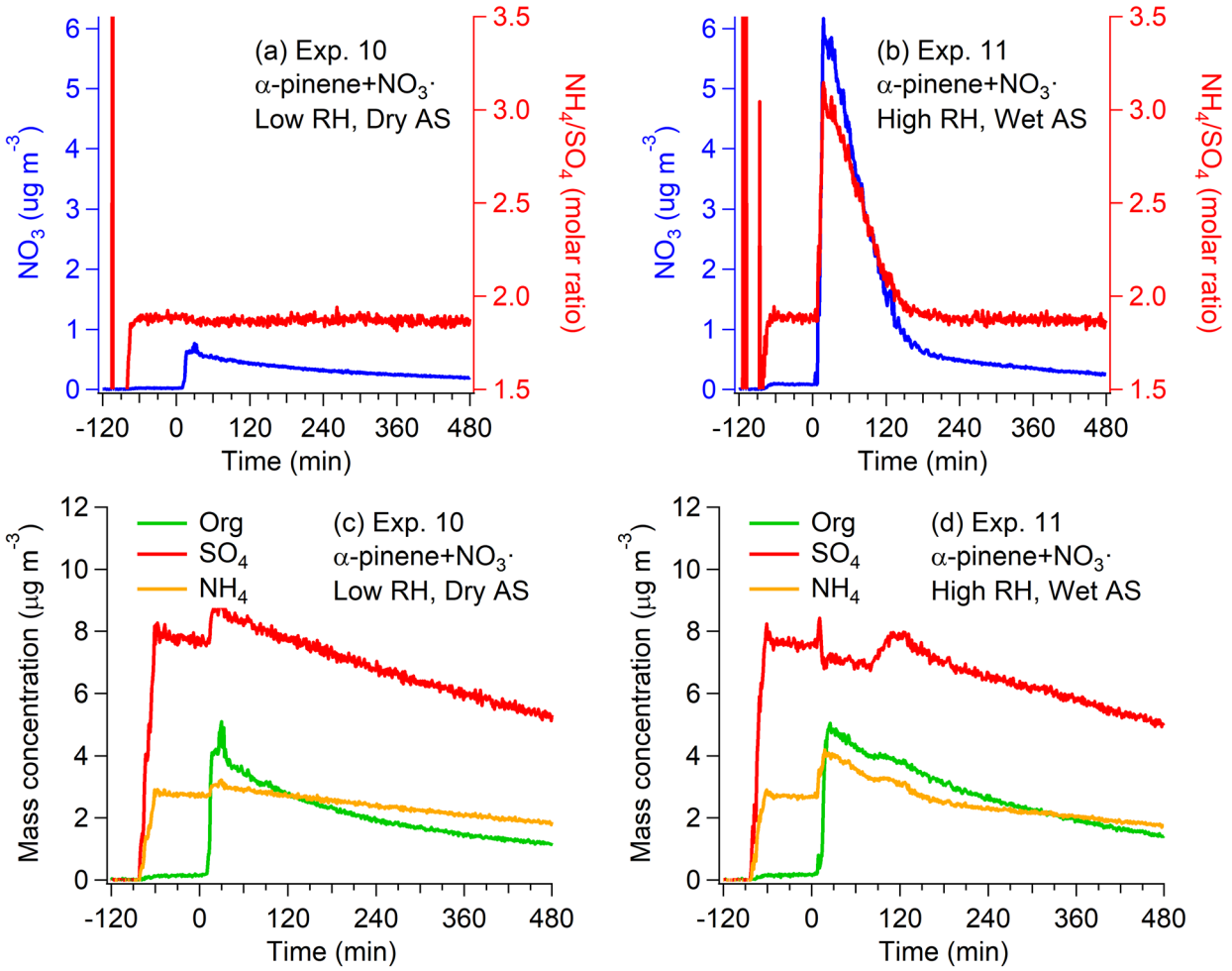

579

580 Figure 2. (a, b) NO_3 concentration and the molar ratio of NH_4 to SO_4 and (c, d) concentrations of Org, SO_4,
581 and NH_4 measured by HR-ToF-AMS. Data presented in Panels (a) and (c) are from Exp. 10 (low RH, dry
582 AS), while those in Panels (b) and (d) are from Exp. 11 (high RH, wet AS). These two experiments are
583 essentially the same except for RH and phase state of seed aerosol.

584

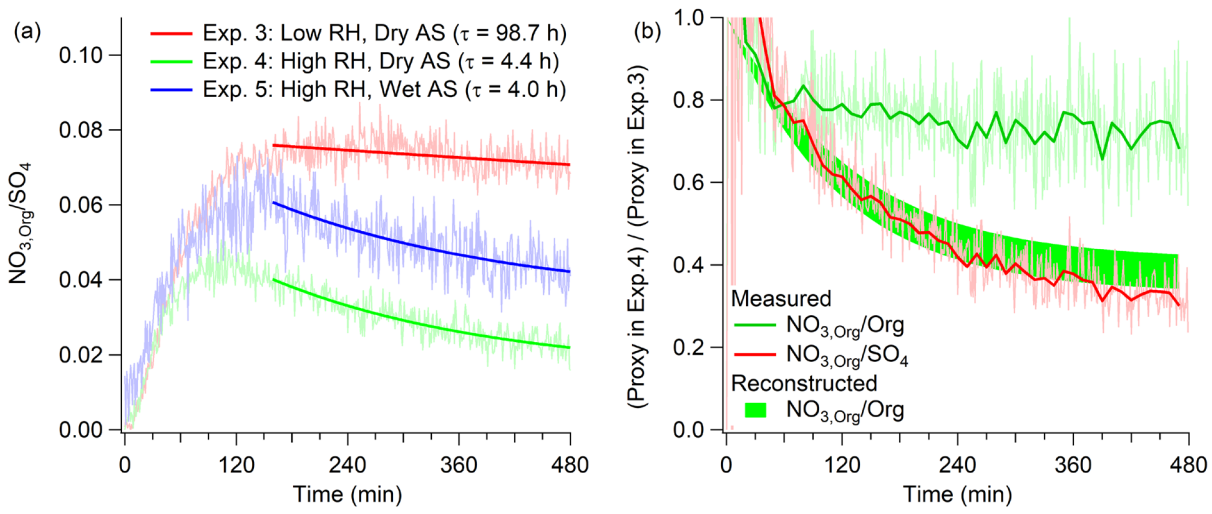

585

586 Figure 3. (a) Time-series data of $NO_{3,Org}/SO_4$ from Exp. 3-5 (α-pinene+OH·) and the exponential fits with
587 corresponding characteristic times. (b) $NO_{3,Org}/Org$, $NO_{3,Org}/SO_4$, reconstructed $NO_{3,Org}/Org$ based on the
588 decay rate of $NO_{3,Org}/SO_4$. Each proxy in Exp. 4 is divided by that in Exp. 3 to determine the relative decay
589 between high and low RH experiments.

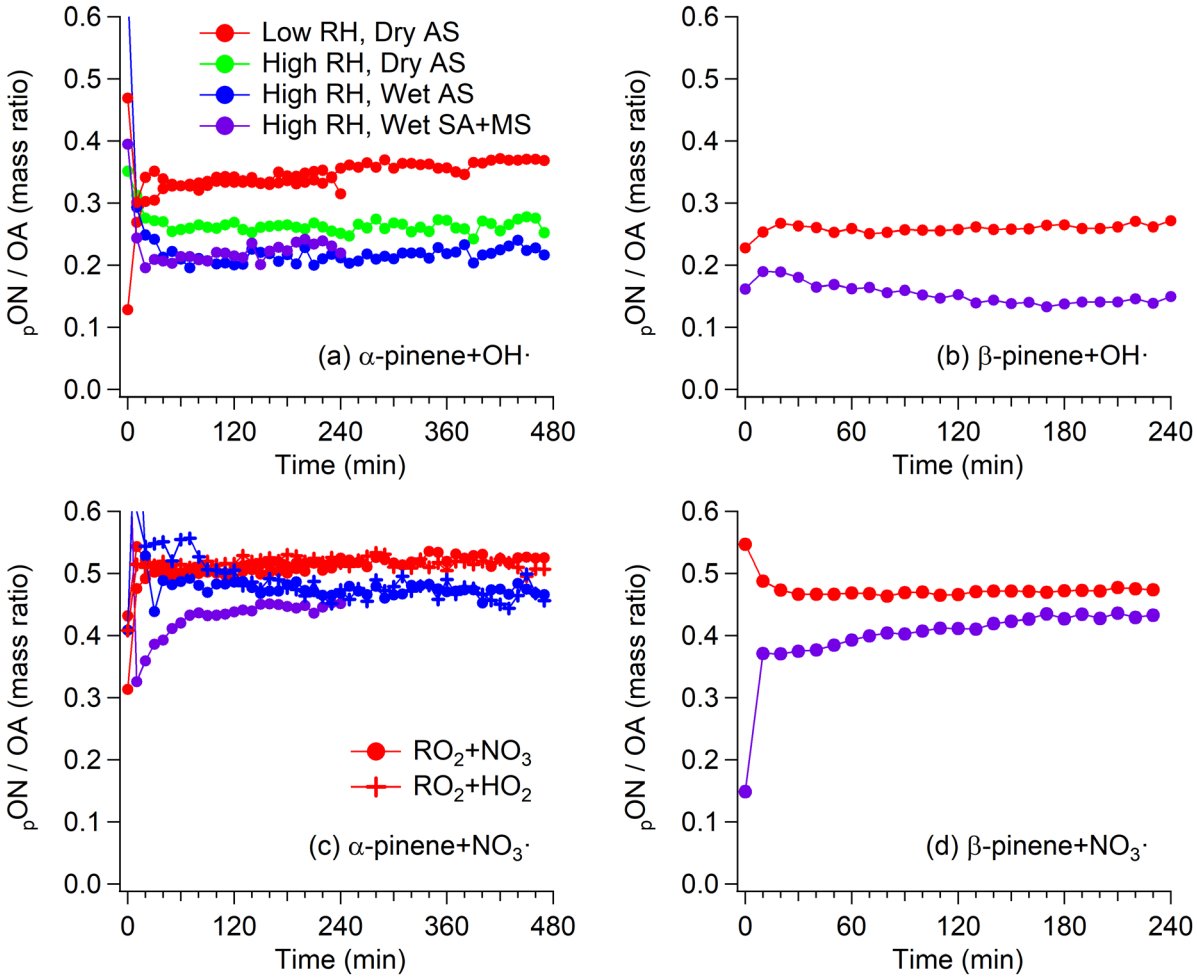

590

591 Figure 4. Time-series data of $_{p}$ON/OA in (a) α-pinene+OH· from Exp. 1-5, (b) β-pinene+OH· from Exp. 6-

592 7, (c) α-pinene+NO_3· from Exp. 8-13, and (d) β-pinene+NO_3· from Exp. 14-15. Data points are colored by

593 conditions concerning reactor RH and phase state of seed aerosol. For α-pinene+NO_3·, data points are also

594 shaped differently depending on the expected dominant RO_2· fate.

595

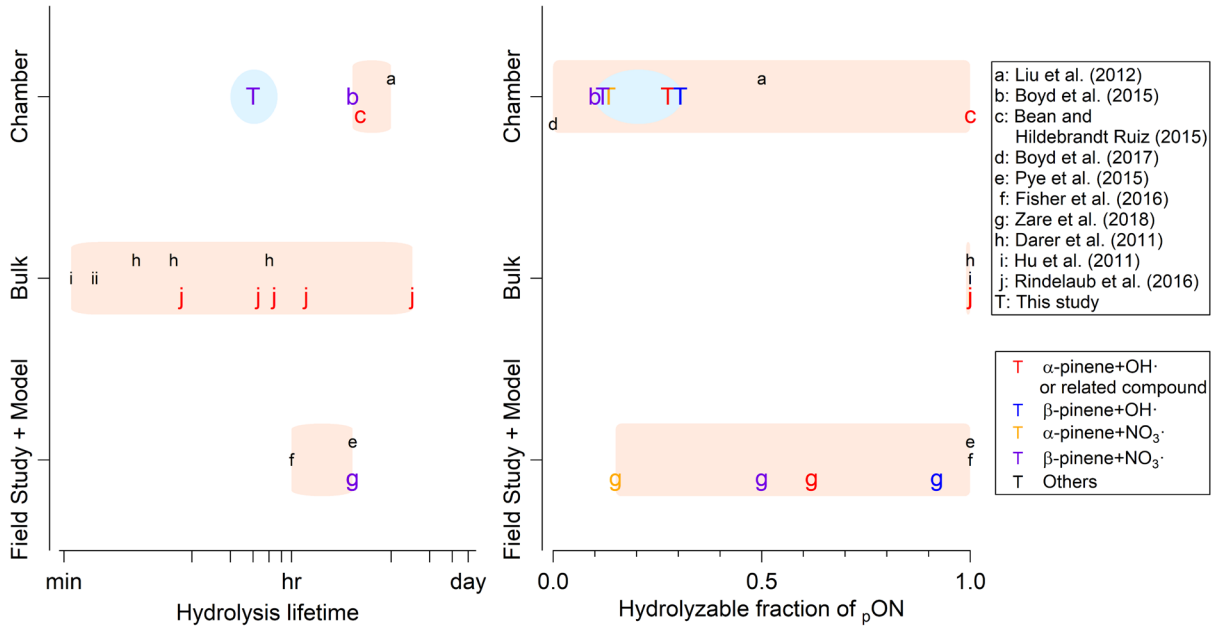

596

597 Figure 5. Comparison of hydrolysis lifetime of organic nitrate and hydrolyzable fraction of $_{p}$ON in
598 literature. “Chamber” refers to laboratory studies of organic nitrate aerosol via chamber experiments,
599 “Bulk” refers to laboratory studies of organic nitrate compounds using bulk solution measurements, and
600 “Model” refers to modeling studies using ambient measurement data as constraints. Data points are colored
601 by the system of VOC and oxidant condition and are alphabetized based on the reference. The relevant
602 systems explored in this study are emphasized by enlarging the corresponding font size. Pink shaded regions
603 are ranges reported in literature, while blue shaded regions are ranges reported in this study.

604

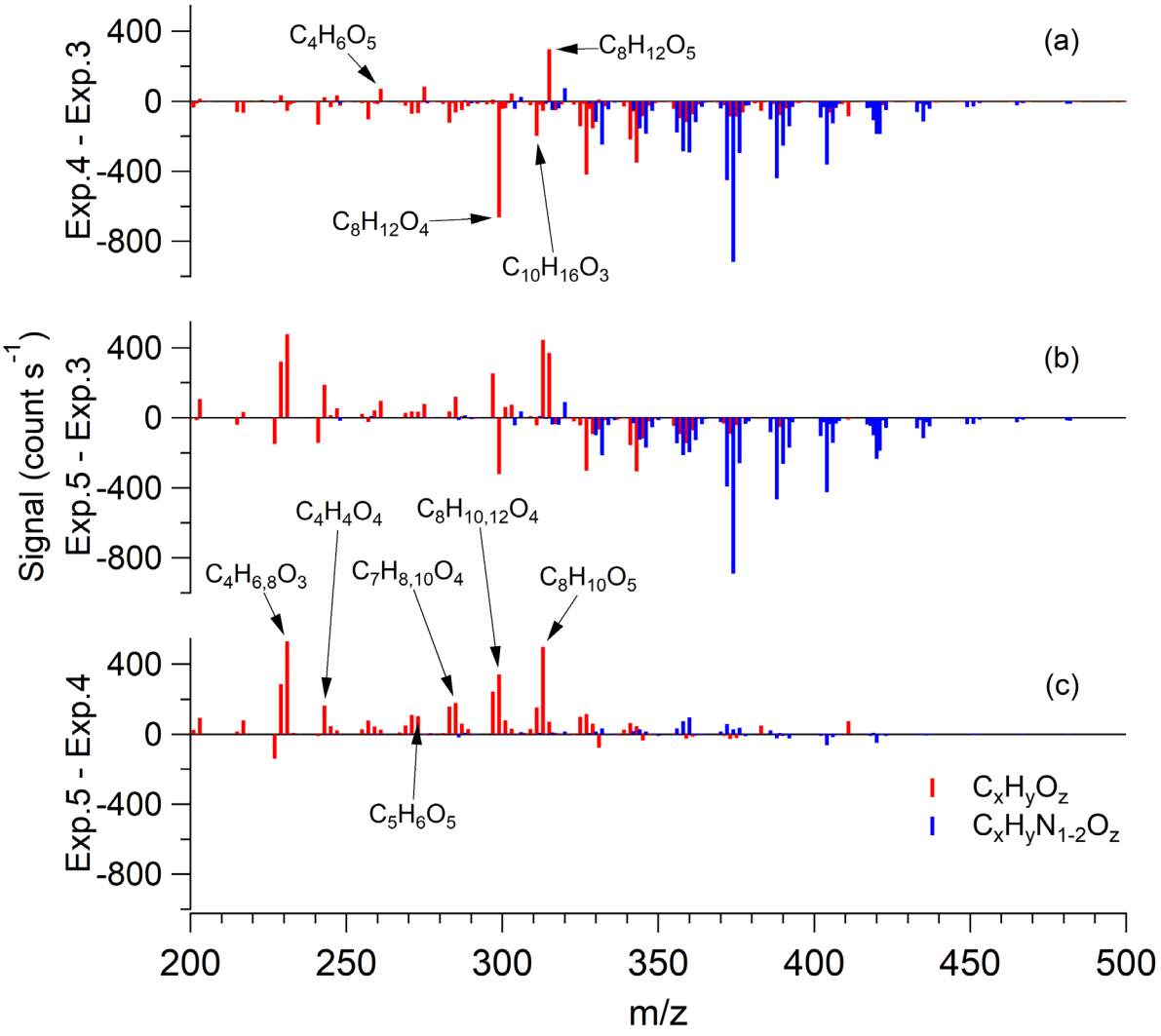

Figure 6. FIGAERO-HR-ToF-I-CIMS difference mass spectra of SOA in α-pinene+OH·. (a) Exp. 4 (high RH, dry AS) minus Exp. 3 (low RH, dry AS). (b) Exp. 5 (high RH, wet AS) minus Exp. 3 (low RH, dry AS). (c) Exp. 5 (high RH, wet AS) minus Exp. 4 (high RH, dry AS). Bars are colored by the difference in chemical composition (i.e., red for $C_xH_yO_z$ and blue for $C_xH_yN_{1-2}O_z$). Prominent masses are labeled with the corresponding chemical formulae without an iodide ion.

613 Table 1. Summary of experimental conditions considered in this study.

Exp.	Precursor VOC	Oxidant precursor	Reactor RH	Seed
1	α-pinene (25 ppb)	H_2O_2 (2 ppm), NO (6 ppb min^{-1})	1-3 %	Effloresced AS[b]
2	α-pinene (25 ppb)	H_2O_2 (2 ppm), NO (6 ppb min^{-1})	48-65 %[a]	Deliquesced SA+MS[c]
3	α-pinene (25 ppb)	H_2O_2 (2 ppm), NO (2 ppb min^{-1})	2-6 %	Effloresced AS
4	α-pinene (25 ppb)	H_2O_2 (2 ppm), NO (2 ppb min^{-1})	53-66 %[a]	Effloresced AS
5	α-pinene (25 ppb)	H_2O_2 (2 ppm), NO (2 ppb min^{-1})	57-72 %[a]	Deliquesced AS
6	β-pinene (25 ppb)	H_2O_2 (2 ppm), NO (6 ppb min^{-1})	1-3 %	Effloresced AS
7	β-pinene (25 ppb)	H_2O_2 (2 ppm), NO (6 ppb min^{-1})	53-70 %[a]	Deliquesced SA+MS
8	α-pinene (12 ppb)	N_2O_5 (80 ppb)	2-3 %	Effloresced AS
9	α-pinene (12 ppb)	N_2O_5 (80 ppb)	67-71 %	Deliquesced SA+MS
10	α-pinene (12 ppb)	N_2O_5 (80 ppb)	1-6 %	Effloresced AS
11	α-pinene (12 ppb)	N_2O_5 (80 ppb)	69-74 %	Deliquesced AS
12	α-pinene (12 ppb)	N_2O_5 (80 ppb), HCHO (25 ppm)	3-8 %	Effloresced AS
13	α-pinene (12 ppb)	N_2O_5 (80 ppb), HCHO (25 ppm)	67-71 %	Deliquesced AS
14	β-pinene (12 ppb)	N_2O_5 (80 ppb)	2-5 %	Effloresced AS
15	β-pinene (12 ppb)	N_2O_5 (80 ppb)	56-72 %	Deliquesced SA+MS

614 [a]The target for the initial reactor RH is ~70 %. However, the irradiation of UV light increases the reactor
615 temperature by several degree Celsius and hence decreases RH.

616 [b]Ammonium sulfate

617 [c]Sulfuric acid and magnesium sulfate

618

619 Table 2. Hydrolysis lifetime and corresponding fraction of hydrolyzable $_{p}$ON.

System	Hydrolysis lifetime	Hydrolyzable fraction (F_H)[a]
α-pinene+OH·	<30 min	23–32 %
β-pinene+OH·	<30 min	27–34 %
α-pinene+NO_3·	<30 min	9–17 %
β-pinene+NO_3·	<30 min	9–15 %

620 [a]Lower or higher limit of hydrolyzable $_{p}$ON fraction is based on the assumptions that organic moiety of
621 hydrolysis products remains in aerosol or partitions back to the gas phase.

622

References

Aljawhary, D., Lee, A. K. Y., and Abbatt, J. P. D.: High-resolution chemical ionization mass spectrometry (ToF-CIMS): application to study SOA composition and processing, Atmos Meas Tech, 6, 3211-3224, 10.5194/amt-6-3211-2013, 2013.

Aljawhary, D., Zhao, R., Lee, A. K. Y., Wang, C., and Abbatt, J. P. D.: Kinetics, Mechanism, and Secondary Organic Aerosol Yield of Aqueous Phase Photo-oxidation of alpha-Pinene Oxidation Products, J Phys Chem A, 120, 1395-1407, 10.1021/acs.jpca.5b06237, 2016.

Aschmann, S. M., Atkinson, R., and Arey, J.: Products of reaction of OH radicals with alpha-pinene, J Geophys Res-Atmos, 107, Artn 4191, 10.1029/2001jd001098, 2002.

Atkinson, R., and Arey, J.: Atmospheric degradation of volatile organic compounds, Chem Rev, 103, 4605-4638, 10.1021/cr0206420, 2003.

Bean, J. K., and Hildebrandt Ruiz, L.: Gas-particle partitioning and hydrolysis of organic nitrates formed from the oxidation of alpha-pinene in environmental chamber experiments, Atmos Chem Phys, 16, 2175-2184, 10.5194/acp-16-2175-2016, 2016.

Berndt, T., and Boge, O.: Products and mechanism of the gas-phase reaction of NO3 radicals with alpha-pinene, J Chem Soc Faraday T, 93, 3021-3027, DOI 10.1039/a702364b, 1997.

Berndt, T., Richters, S., Jokinen, T., Hyttinen, N., Kurten, T., Otkjaer, R. V., Kjaergaard, H. G., Stratmann, F., Herrmann, H., Sipila, M., Kulmala, M., and Ehn, M.: Hydroxyl radical-induced formation of highly oxidized organic compounds, Nat Commun, 7, 10.1038/ncomms13677, 2016.

Bertram, T. H., Kimmel, J. R., Crisp, T. A., Ryder, O. S., Yatavelli, R. L. N., Thornton, J. A., Cubison, M. J., Gonin, M., and Worsnop, D. R.: A field-deployable, chemical ionization time-of-flight mass spectrometer, Atmos Meas Tech, 4, 1471-1479, 10.5194/amt-4-1471-2011, 2011.

Boschan, R., Merrow, R. T., and Vandolah, R. W.: The Chemistry of Nitrate Esters, Chem Rev, 55, 485-510, DOI 10.1021/cr50003a001, 1955.

Boyd, C. M., Sanchez, J., Xu, L., Eugene, A. J., Nah, T., Tuet, W. Y., Guzman, M. I., and Ng, N. L.: Secondary organic aerosol formation from the beta-pinene+NO3 system: effect of humidity and peroxy radical fate, Atmos Chem Phys, 15, 7497-7522, 10.5194/acp-15-7497-2015, 2015.

Boyd, C. M., Nah, T., Xu, L., Berkemeier, T., and Ng, N. L.: Secondary Organic Aerosol (SOA) from Nitrate Radical Oxidation of Monoterpenes: Effects of Temperature, Dilution, and Humidity on Aerosol Formation, Mixing, and Evaporation, Environ Sci Technol, 51, 7831-7841, 10.1021/acs.est.7b01460, 2017.

Browne, E. C., Min, K. E., Wooldridge, P. J., Apel, E., Blake, D. R., Brune, W. H., Cantrell, C. A., Cubison, M. J., Diskin, G. S., Jimenez, J. L., Weinheimer, A. J., Wennberg, P. O., Wisthaler, A., and Cohen, R. C.: Observations of total RONO2 over the boreal forest: NOx sinks and HNO3 sources, Atmos Chem Phys, 13, 4543-4562, 10.5194/acp-13-4543-2013, 2013.

Bruns, E. A., Perraud, V., Zelenyuk, A., Ezell, M. J., Johnson, S. N., Yu, Y., Imre, D., Finlayson-Pitts, B. J., and Alexander, M. L.: Comparison of FTIR and Particle Mass Spectrometry for the Measurement of Particulate Organic Nitrates, Environ Sci Technol, 44, 1056-1061, 10.1021/es9029864, 2010.

660 Canagaratna, M. R., Jimenez, J. L., Kroll, J. H., Chen, Q., Kessler, S. H., Massoli, P., Hildebrandt Ruiz, L.,
661 Fortner, E., Williams, L. R., Wilson, K. R., Surratt, J. D., Donahue, N. M., Jayne, J. T., and Worsnop, D.
662 R.: Elemental ratio measurements of organic compounds using aerosol mass spectrometry: characterization,
663 improved calibration, and implications, Atmos Chem Phys, 15, 253-272, 10.5194/acp-15-253-2015, 2015.

664 Carlton, A. G., Pinder, R. W., Bhave, P. V., and Pouliot, G. A.: To What Extent Can Biogenic SOA be
665 Controlled?, Environ Sci Technol, 44, 3376-3380, 10.1021/es903506b, 2010.

666 Cerully, K. M., Bougiatioti, A., Hite, J. R., Guo, H., Xu, L., Ng, N. L., Weber, R., and Nenes, A.: On the
667 link between hygroscopicity, volatility, and oxidation state of ambient and water-soluble aerosols in the
668 southeastern United States, Atmos Chem Phys, 15, 8679-8694, 10.5194/acp-15-8679-2015, 2015.

669 Claflin, M. S., and Ziemann, P. J.: Identification and Quantitation of Aerosol Products of the Reaction of
670 beta-Pinene with NO3 Radicals and Implications for Gas- and Particle-Phase Reaction Mechanisms, J Phys
671 Chem A, 122, 3640-3652, 10.1021/acs.jpca.8b00692, 2018.

672 Crounse, J. D., Nielsen, L. B., Jorgensen, S., Kjaergaard, H. G., and Wennberg, P. O.: Autoxidation of
673 Organic Compounds in the Atmosphere, J Phys Chem Lett, 4, 3513-3520, 10.1021/jz4019207, 2013.

674 Darer, A. I., Cole-Filipiak, N. C., O'Connor, A. E., and Elrod, M. J.: Formation and Stability of
675 Atmospherically Relevant Isoprene-Derived Organosulfates and Organonitrates, Environ Sci Technol, 45,
676 1895-1902, 10.1021/es103797z, 2011.

677 Day, D. A., Liu, S., Russell, L. M., and Ziemann, P. J.: Organonitrate group concentrations in submicron
678 particles with high nitrate and organic fractions in coastal southern California, Atmos Environ, 44, 1970-
679 1979, 10.1016/j.atmosenv.2010.02.045, 2010.

680 DeCarlo, P. F., Kimmel, J. R., Trimborn, A., Northway, M. J., Jayne, J. T., Aiken, A. C., Gonin, M., Fuhrer,
681 K., Horvath, T., Docherty, K. S., Worsnop, D. R., and Jimenez, J. L.: Field-deployable, high-resolution,
682 time-of-flight aerosol mass spectrometer, Anal Chem, 78, 8281-8289, 10.1021/ac061249n, 2006.

683 Eddingsaas, N. C., Loza, C. L., Yee, L. D., Chan, M., Schilling, K. A., Chhabra, P. S., Seinfeld, J. H., and
684 Wennberg, P. O.: alpha-pinene photooxidation under controlled chemical conditions - Part 2: SOA yield
685 and composition in low- and high-NOx environments, Atmos Chem Phys, 12, 7413-7427, 10.5194/acp-12-
686 7413-2012, 2012.

687 Ehn, M., Thornton, J. A., Kleist, E., Sipila, M., Junninen, H., Pullinen, I., Springer, M., Rubach, F.,
688 Tillmann, R., Lee, B., Lopez-Hilfiker, F., Andres, S., Acir, I. H., Rissanen, M., Jokinen, T., Schobesberger,
689 S., Kangasluoma, J., Kontkanen, J., Nieminen, T., Kurten, T., Nielsen, L. B., Jorgensen, S., Kjaergaard, H.
690 G., Canagaratna, M., Dal Maso, M., Berndt, T., Petaja, T., Wahner, A., Kerminen, V. M., Kulmala, M.,
691 Worsnop, D. R., Wildt, J., and Mentel, T. F.: A large source of low-volatility secondary organic aerosol,
692 Nature, 506, 476-+, 10.1038/nature13032, 2014.

693 Ervens, B., Turpin, B. J., and Weber, R. J.: Secondary organic aerosol formation in cloud droplets and
694 aqueous particles (aqSOA): a review of laboratory, field and model studies, Atmos Chem Phys, 11, 11069-
695 11102, 10.5194/acp-11-11069-2011, 2011.

696 Farmer, D. K., Matsunaga, A., Docherty, K. S., Surratt, J. D., Seinfeld, J. H., Ziemann, P. J., and Jimenez,
697 J. L.: Response of an aerosol mass spectrometer to organonitrates and organosulfates and implications for
698 atmospheric chemistry, P Natl Acad Sci USA, 107, 6670-6675, 10.1073/pnas.0912340107, 2010.

699 Faxon, C., Hammes, J., Le Breton, M., Pathak, R. K., and Hallquist, M.: Characterization of organic nitrate
700 constituents of secondary organic aerosol (SOA) from nitrate-radical-initiated oxidation of limonene using
701 high-resolution chemical ionization mass spectrometry, Atmos Chem Phys, 18, 5467-5481, 10.5194/acp-
702 18-5467-2018, 2018.

703 Fisher, J. A., Jacob, D. J., Travis, K. R., Kim, P. S., Marais, E. A., Miller, C. C., Yu, K. R., Zhu, L.,
704 Yantosca, R. M., Sulprizio, M. P., Mao, J. Q., Wennberg, P. O., Crounse, J. D., Teng, A. P., Nguyen, T. B.,
705 St Clair, J. M., Cohen, R. C., Romer, P., Nault, B. A., Wooldridge, P. J., Jimenez, J. L., Campuzano-Jost,
706 P., Day, D. A., Hu, W. W., Shepson, P. B., Xiong, F. L. Z., Blake, D. R., Goldstein, A. H., Misztal, P. K.,
707 Hanisco, T. F., Wolfe, G. M., Ryerson, T. B., Wisthaler, A., and Mikoviny, T.: Organic nitrate chemistry
708 and its implications for nitrogen budgets in an isoprene- and monoterpene-rich atmosphere: constraints
709 from aircraft (SEAC(4)RS) and ground-based (SOAS) observations in the Southeast US, Atmos Chem
710 Phys, 16, 5969-5991, 10.5194/acp-16-5969-2016, 2016.

711 Fry, J. L., Kiendler-Scharr, A., Rollins, A. W., Wooldridge, P. J., Brown, S. S., Fuchs, H., Dube, W.,
712 Mensah, A., dal Maso, M., Tillmann, R., Dorn, H. P., Brauers, T., and Cohen, R. C.: Organic nitrate and
713 secondary organic aerosol yield from NO3 oxidation of beta-pinene evaluated using a gas-phase
714 kinetics/aerosol partitioning model, Atmos Chem Phys, 9, 1431-1449, DOI 10.5194/acp-9-1431-2009,
715 2009.

716 Fry, J. L., Draper, D. C., Zarzana, K. J., Campuzano-Jost, P., Day, D. A., Jimenez, J. L., Brown, S. S.,
717 Cohen, R. C., Kaser, L., Hansel, A., Cappellin, L., Karl, T., Roux, A. H., Turnipseed, A., Cantrell, C., Lefer,
718 B. L., and Grossberg, N.: Observations of gas- and aerosol-phase organic nitrates at BEACHON-RoMBAS
719 2011, Atmos Chem Phys, 13, 8585-8605, 10.5194/acp-13-8585-2013, 2013.

720 Fry, J. L., Draper, D. C., Barsanti, K. C., Smith, J. N., Ortega, J., Winkle, P. M., Lawler, M. J., Brown, S.
721 S., Edwards, P. M., Cohen, R. C., and Lee, L.: Secondary Organic Aerosol Formation and Organic Nitrate
722 Yield from NO3 Oxidation of Biogenic Hydrocarbons, Environ Sci Technol, 48, 11944-11953,
723 10.1021/es502204x, 2014.

724 Fry, J. L., Brown, S. S., Middlebrook, A. M., Edwards, P. M., Campuzano-Jost, P., Day, D. A., Jimenez, J.
725 L., Allen, H. M., Ryerson, T. B., Pollack, I., Graus, M., Warneke, C., de Gouw, J. A., Brock, C. A., Gilman,
726 J., Lerner, B. M., Dube, W. P., Liao, J., and Welti, A.: Secondary organic aerosol (SOA) yields from NO3
727 radical + isoprene based on nighttime aircraft power plant plume transects, Atmos Chem Phys, 18, 11663-
728 11682, 10.5194/acp-18-11663-2018, 2018.

729 Gao, S., Ng, N. L., Keywood, M., Varutbangkul, V., Bahreini, R., Nenes, A., He, J. W., Yoo, K. Y.,
730 Beauchamp, J. L., Hodyss, R. P., Flagan, R. C., and Seinfeld, J. H.: Particle phase acidity and oligomer
731 formation in secondary organic aerosol, Environ Sci Technol, 38, 6582-6589, 10.1021/es049125k, 2004.

732 Goldstein, A. H., and Galbally, I. E.: Known and unexplored organic constituents in the earth's atmosphere,
733 Environ Sci Technol, 41, 1514-1521, DOI 10.1021/es072476p, 2007.

734 Griffin, R. J., Cocker, D. R., Flagan, R. C., and Seinfeld, J. H.: Organic aerosol formation from the oxidation
735 of biogenic hydrocarbons, J Geophys Res-Atmos, 104, 3555-3567, Doi 10.1029/1998jd100049, 1999.

736 Grzinic, G., Bartels-Rausch, T., Berkemeier, T., Turler, A., and Ammann, M.: Viscosity controls humidity
737 dependence of N2O5 uptake to citric acid aerosol, Atmos Chem Phys, 15, 13615-13625, 10.5194/acp-15-
738 13615-2015, 2015.

739 Guenther, A. B., Jiang, X., Heald, C. L., Sakulyanontvittaya, T., Duhl, T., Emmons, L. K., and Wang, X.:
740 The Model of Emissions of Gases and Aerosols from Nature version 2.1 (MEGAN2.1): an extended and
741 updated framework for modeling biogenic emissions, Geosci Model Dev, 5, 1471-1492, 10.5194/gmd-5-
742 1471-2012, 2012.

743 Hallquist, M., Wangberg, I., Ljungstrom, E., Barnes, I., and Becker, K. H.: Aerosol and product yields from
744 NO3 radical-initiated oxidation of selected monoterpenes, Environ Sci Technol, 33, 553-559, DOI
745 10.1021/es980292s, 1999.

746 Hoyle, C. R., Boy, M., Donahue, N. M., Fry, J. L., Glasius, M., Guenther, A., Hallar, A. G., Hartz, K. H.,
747 Petters, M. D., Petaja, T., Rosenoern, T., and Sullivan, A. P.: A review of the anthropogenic influence on
748 biogenic secondary organic aerosol, Atmos Chem Phys, 11, 321-343, 10.5194/acp-11-321-2011, 2011.

749 Hu, K. S., Darer, A. I., and Elrod, M. J.: Thermodynamics and kinetics of the hydrolysis of atmospherically
750 relevant organonitrates and organosulfates, Atmos Chem Phys, 11, 8307-8320, 10.5194/acp-11-8307-2011,
751 2011.

752 Huang, W., Saathoff, H., Shen, X. L., Ramisetty, R., Leisner, T., and Mohr, C.: Chemical Characterization
753 of Highly Functionalized Organonitrates Contributing to Night-Time Organic Aerosol Mass Loadings and
754 Particle Growth, Environ Sci Technol, 53, 1165-1174, 10.1021/acs.est.8b05826, 2019.

755 Huang, Y. L., Zhao, R., Charan, S. M., Kenseth, C. M., Zhang, X., and Seinfeld, J. H.: Unified Theory of
756 Vapor-Wall Mass Transport in Teflon-Walled Environmental Chambers, Environ Sci Technol, 52, 2134-
757 2142, 10.1021/acs.est.7b05575, 2018.

758 Jacobs, M. I., Burke, W. J., and Elrod, M. J.: Kinetics of the reactions of isoprene-derived hydroxynitrates:
759 gas phase epoxide formation and solution phase hydrolysis, Atmos Chem Phys, 14, 8933-8946,
760 10.5194/acp-14-8933-2014, 2014.

761 Jenkin, M. E., Saunders, S. M., and Pilling, M. J.: The tropospheric degradation of volatile organic
762 compounds: A protocol for mechanism development, Atmos Environ, 31, 81-104, Doi 10.1016/S1352-
763 2310(96)00105-7, 1997.

764 Jokinen, T., Berndt, T., Makkonen, R., Kerminen, V. M., Junninen, H., Paasonen, P., Stratmann, F.,
765 Herrmann, H., Guenther, A. B., Worsnop, D. R., Kulmala, M., Ehn, M., and Sipila, M.: Production of
766 extremely low volatile organic compounds from biogenic emissions: Measured yields and atmospheric
767 implications, P Natl Acad Sci USA, 112, 7123-7128, 10.1073/pnas.1423977112, 2015.

768 Kanakidou, M., Seinfeld, J. H., Pandis, S. N., Barnes, I., Dentener, F. J., Facchini, M. C., Van Dingenen,
769 R., Ervens, B., Nenes, A., Nielsen, C. J., Swietlicki, E., Putaud, J. P., Balkanski, Y., Fuzzi, S., Horth, J.,
770 Moortgat, G. K., Winterhalter, R., Myhre, C. E. L., Tsigaridis, K., Vignati, E., Stephanou, E. G., and
771 Wilson, J.: Organic aerosol and global climate modelling: a review, Atmos Chem Phys, 5, 1053-1123, DOI
772 10.5194/acp-5-1053-2005, 2005.

773 Kebabian, P. L., Herndon, S. C., and Freedman, A.: Detection of nitrogen dioxide by cavity attenuated
774 phase shift spectroscopy, Anal Chem, 77, 724-728, 10.1021/ac048715y, 2005.

775 Kiendler-Scharr, A., Mensah, A. A., Friese, E., Topping, D., Nemitz, E., Prevot, A. S. H., Aijala, M., Allan,
776 J., Canonaco, F., Canagaratna, M., Carbone, S., Crippa, M., Dall Osto, M., Day, D. A., De Carlo, P., Di
777 Marco, C. F., Elbern, H., Eriksson, A., Freney, E., Hao, L., Herrmann, H., Hildebrandt, L., Hillamo, R.,
778 Jimenez, J. L., Laaksonen, A., McFiggans, G., Mohr, C., O'Dowd, C., Otjes, R., Ovadnevaite, J., Pandis, S.

N., Poulain, L., Schlag, P., Sellegri, K., Swietlicki, E., Tiitta, P., Vermeulen, A., Wahner, A., Worsnop, D., and Wu, H. C.: Ubiquity of organic nitrates from nighttime chemistry in the European submicron aerosol, Geophys Res Lett, 43, 7735-7744, 10.1002/2016gl069239, 2016.

Krechmer, J. E., Pagonis, D., Ziemann, P. J., and Jimenez, J. L.: Quantification of Gas-Wall Partitioning in Teflon Environmental Chambers Using Rapid Bursts of Low-Volatility Oxidized Species Generated in Situ, Environ Sci Technol, 50, 5757-5765, 10.1021/acs.est.6b00606, 2016.

Kroll, J. H., and Seinfeld, J. H.: Chemistry of secondary organic aerosol: Formation and evolution of low-volatility organics in the atmosphere, Atmos Environ, 42, 3593-3624, 10.1016/j.atmosenv.2008.01.003, 2008.

Kurten, T., Moller, K. H., Nguyen, T. B., Schwantes, R. H., Misztal, P. K., Su, L. P., Wennberg, P. O., Fry, J. L., and Kjaergaard, H. G.: Alkoxy Radical Bond Scissions Explain the Anomalously Low Secondary Organic Aerosol and Organonitrate Yields From alpha-Pinene + NO3, J Phys Chem Lett, 8, 2826-2834, 10.1021/acs.jpclett.7b01038, 2017.

La, Y. S., Camredon, M., Ziemann, P. J., Valorso, R., Matsunaga, A., Lannuque, V., Lee-Taylor, J., Hodzic, A., Madronich, S., and Aumont, B.: Impact of chamber wall loss of gaseous organic compounds on secondary organic aerosol formation: explicit modeling of SOA formation from alkane and alkene oxidation, Atmos Chem Phys, 16, 1417-1431, 10.5194/acp-16-1417-2016, 2016.

Lee, B. H., Lopez-Hilfiker, F. D., Mohr, C., Kurten, T., Worsnop, D. R., and Thornton, J. A.: An Iodide-Adduct High-Resolution Time-of-Flight Chemical-Ionization Mass Spectrometer: Application to Atmospheric Inorganic and Organic Compounds, Environ Sci Technol, 48, 6309-6317, 10.1021/es500362a, 2014.

Lee, B. H., Mohr, C., Lopez-Hilfiker, F. D., Lutz, A., Hallquist, M., Lee, L., Romer, P., Cohen, R. C., Iyer, S., Kurten, T., Hu, W. W., Day, D. A., Campuzano-Jost, P., Jimenez, J. L., Xu, L., Ng, N. L., Guo, H. Y., Weber, R. J., Wild, R. J., Brown, S. S., Koss, A., de Gouw, J., Olson, K., Goldstein, A. H., Seco, R., Kim, S., McAvey, K., Shepson, P. B., Starn, T., Baumann, K., Edgerton, E. S., Liu, J. M., Shilling, J. E., Miller, D. O., Brune, W., Schobesberger, S., D'Ambro, E. L., and Thornton, J. A.: Highly functionalized organic nitrates in the southeast United States: Contribution to secondary organic aerosol and reactive nitrogen budgets, P Natl Acad Sci USA, 113, 1516-1521, 10.1073/pnas.1508108113, 2016.

Liggio, J., and Li, S. M.: Reactive uptake of pinonaldehyde on acidic aerosols, J Geophys Res-Atmos, 111, Artn D24303, 10.1029/2005jd006978, 2006.

Liggio, J., and Li, S. M.: Reversible and irreversible processing of biogenic olefins on acidic aerosols, Atmos Chem Phys, 8, 2039-2055, DOI 10.5194/acp-8-2039-2008, 2008.

Liu, S., Ahlm, L., Day, D. A., Russell, L. M., Zhao, Y. L., Gentner, D. R., Weber, R. J., Goldstein, A. H., Jaoui, M., Offenberg, J. H., Kleindienst, T. E., Rubitschun, C., Surratt, J. D., Sheesley, R. J., and Scheller, S.: Secondary organic aerosol formation from fossil fuel sources contribute majority of summertime organic mass at Bakersfield, J Geophys Res-Atmos, 117, Artn D00v26, 10.1029/2012jd018170, 2012a.

Liu, S., Shilling, J. E., Song, C., Hiranuma, N., Zaveri, R. A., and Russell, L. M.: Hydrolysis of Organonitrate Functional Groups in Aerosol Particles, Aerosol Sci Tech, 46, 1359-1369, 10.1080/02786826.2012.716175, 2012b.

Lopez-Hilfiker, F. D., Mohr, C., Ehn, M., Rubach, F., Kleist, E., Wildt, J., Mentel, T. F., Lutz, A., Hallquist, M., Worsnop, D., and Thornton, J. A.: A novel method for online analysis of gas and particle composition:

description and evaluation of a Filter Inlet for Gases and AEROsols (FIGAERO), Atmos Meas Tech, 7, 983-1001, 10.5194/amt-7-983-2014, 2014.

Loza, C. L., Chan, A. W. H., Galloway, M. M., Keutsch, F. N., Flagan, R. C., and Seinfeld, J. H.: Characterization of Vapor Wall Loss in Laboratory Chambers, Environ Sci Technol, 44, 5074-5078, 10.1021/es100727v, 2010.

Matsunaga, A., and Ziemann, P. J.: Gas-Wall Partitioning of Organic Compounds in a Teflon Film Chamber and Potential Effects on Reaction Product and Aerosol Yield Measurements, Aerosol Sci Tech, 44, 881-892, 10.1080/02786826.2010.501044, 2010.

Mcvay, R. C., Cappa, C. D., and Seinfeld, J. H.: Vapor-Wall Deposition in Chambers: Theoretical Considerations, Environ Sci Technol, 48, 10251-10258, 10.1021/es502170j, 2014.

Muller, J. F., Peeters, J., and Stavrakou, T.: Fast photolysis of carbonyl nitrates from isoprene, Atmos Chem Phys, 14, 2497-2508, 10.5194/acp-14-2497-2014, 2014.

Nah, T., Sanchez, J., Boyd, C. M., and Ng, N. L.: Photochemical Aging of alpha-pinene and beta-pinene Secondary Organic Aerosol formed from Nitrate Radical Oxidation, Environ Sci Technol, 50, 222-231, 10.1021/acs.est.5b04594, 2016.

Ng, N. L., Herndon, S. C., Trimborn, A., Canagaratna, M. R., Croteau, P. L., Onasch, T. B., Sueper, D., Worsnop, D. R., Zhang, Q., Sun, Y. L., and Jayne, J. T.: An Aerosol Chemical Speciation Monitor (ACSM) for Routine Monitoring of the Composition and Mass Concentrations of Ambient Aerosol, Aerosol Sci Tech, 45, 780-794, Pii 934555189, 10.1080/02786826.2011.560211, 2011.

Ng, N. L., Brown, S. S., Archibald, A. T., Atlas, E., Cohen, R. C., Crowley, J. N., Day, D. A., Donahue, N. M., Fry, J. L., Fuchs, H., Griffin, R. J., Guzman, M. I., Herrmann, H., Hodzic, A., Iinuma, Y., Jimenez, J. L., Kiendler-Scharr, A., Lee, B. H., Luecken, D. J., Mao, J. Q., McLaren, R., Mutzel, A., Osthoff, H. D., Ouyang, B., Picquet-Varrault, B., Platt, U., Pye, H. O. T., Rudich, Y., Schwantes, R. H., Shiraiwa, M., Stutz, J., Thornton, J. A., Tilgner, A., Williams, B. J., and Zaveri, R. A.: Nitrate radicals and biogenic volatile organic compounds: oxidation, mechanisms, and organic aerosol, Atmos Chem Phys, 17, 2103-2162, 10.5194/acp-17-2103-2017, 2017.

Nguyen, T. B., Crounse, J. D., Teng, A. P., Clair, J. M. S., Paulot, F., Wolfe, G. M., and Wennberg, P. O.: Rapid deposition of oxidized biogenic compounds to a temperate forest, P Natl Acad Sci USA, 112, E392-E401, 10.1073/pnas.1418702112, 2015.

Noziere, B., Barnes, I., and Becker, K. H.: Product study and mechanisms of the reactions of alpha-pinene and of pinonaldehyde with OH radicals, J Geophys Res-Atmos, 104, 23645-23656, Doi 10.1029/1999jd900778, 1999.

Orlando, J. J., and Tyndall, G. S.: Laboratory studies of organic peroxy radical chemistry: an overview with emphasis on recent issues of atmospheric significance, Chem Soc Rev, 41, 6294-6317, 10.1039/c2cs35166h, 2012.

Pankow, J. F.: An Absorption-Model of Gas-Particle Partitioning of Organic-Compounds in the Atmosphere, Atmos Environ, 28, 185-188, Doi 10.1016/1352-2310(94)90093-0, 1994.

Pankow, J. F., and Asher, W. E.: SIMPOL.1: a simple group contribution method for predicting vapor pressures and enthalpies of vaporization of multifunctional organic compounds, Atmos Chem Phys, 8, 2773-2796, DOI 10.5194/acp-8-2773-2008, 2008.

Perring, A. E., Pusede, S. E., and Cohen, R. C.: An Observational Perspective on the Atmospheric Impacts of Alkyl and Multifunctional Nitrates on Ozone and Secondary Organic Aerosol, Chem Rev, 113, 5848-5870, 10.1021/cr300520x, 2013.

Petters, M. D., and Kreidenweis, S. M.: A single parameter representation of hygroscopic growth and cloud condensation nucleus activity, Atmos Chem Phys, 7, 1961-1971, DOI 10.5194/acp-7-1961-2007, 2007.

Pye, H. O. T., Luecken, D. J., Xu, L., Boyd, C. M., Ng, N. L., Baker, K. R., Ayres, B. R., Bash, J. O., Baumann, K., Carter, W. P. L., Edgerton, E., Fry, J. L., Hutzell, W. T., Schwede, D. B., and Shepson, P. B.: Modeling the Current and Future Roles of Particulate Organic Nitrates in the Southeastern United States, Environ Sci Technol, 49, 14195-14203, 10.1021/acs.est.5b03738, 2015.

Pye, H. O. T., D'Ambro, E. L., Lee, B., Schobesberger, S., Takeuchi, M., Zhao, Y., Lopez-Hilfiker, F., Liu, J. M., Shilling, J. E., Xing, J., Mathur, R., Middlebrook, A. M., Liao, J., Welti, A., Graus, M., Warneke, C., de Gouw, J. A., Holloway, J. S., Ryerson, T. B., Pollack, I. B., and Thornton, J. A.: Anthropogenic enhancements to production of highly oxygenated molecules from autoxidation, P Natl Acad Sci USA, 116, 6641-6646, 10.1073/pnas.1810774116, 2019.

Rindelaub, J. D., McAvey, K. M., and Shepson, P. B.: The photochemical production of organic nitrates from alpha-pinene and loss via acid-dependent particle phase hydrolysis, Atmos Environ, 100, 193-201, 2015.

Rindelaub, J. D., Borca, C. H., Hostetler, M. A., Slade, J. H., Lipton, M. A., Slipchenko, L. V., and Shepson, P. B.: The acid-catalyzed hydrolysis of an alpha-pinene-derived organic nitrate: kinetics, products, reaction mechanisms, and atmospheric impact, Atmos Chem Phys, 16, 15425-15432, 10.5194/acp-16-15425-2016, 2016.

Rollins, A. W., Browne, E. C., Min, K. E., Pusede, S. E., Wooldridge, P. J., Gentner, D. R., Goldstein, A. H., Liu, S., Day, D. A., Russell, L. M., and Cohen, R. C.: Evidence for NOx Control over Nighttime SOA Formation, Science, 337, 1210-1212, 10.1126/science.1221520, 2012.

Rollins, A. W., Pusede, S., Wooldridge, P., Min, K. E., Gentner, D. R., Goldstein, A. H., Liu, S., Day, D. A., Russell, L. M., Rubitschun, C. L., Surratt, J. D., and Cohen, R. C.: Gas/particle partitioning of total alkyl nitrates observed with TD-LIF in Bakersfield, J Geophys Res-Atmos, 118, 6651-6662, 10.1002/jgrd.50522, 2013.

Romonosky, D. E., Li, Y., Shiraiwa, M., Laskin, A., Laskin, J., and Nizkorodov, S. A.: Aqueous Photochemistry of Secondary Organic Aerosol of alpha-Pinene and alpha-Humulene Oxidized with Ozone, Hydroxyl Radical, and Nitrate Radical, J Phys Chem A, 121, 1298-1309, 10.1021/acs.jpca.6b10900, 2017.

Ruggeri, G., Bernhard, F. A., Henderson, B. H., and Takahama, S.: Model-measurement comparison of functional group abundance in alpha-pinene and 1,3,5-trimethylbenzene secondary organic aerosol formation, Atmos Chem Phys, 16, 8729-8747, 10.5194/acp-16-8729-2016, 2016.

Russell, L. M., Bahadur, R., and Ziemann, P. J.: Identifying organic aerosol sources by comparing functional group composition in chamber and atmospheric particles, P Natl Acad Sci USA, 108, 3516-3521, 10.1073/pnas.1006461108, 2011.

Sanchez, J., Tanner, D. J., Chen, D. X., Huey, L. G., and Ng, N. L.: A new technique for the direct detection of HO2 radicals using bromide chemical ionization mass spectrometry (Br-CIMS): initial characterization, Atmos Meas Tech, 9, 3851-3861, 10.5194/amt-9-3851-2016, 2016.

Saunders, S. M., Jenkin, M. E., Derwent, R. G., and Pilling, M. J.: Protocol for the development of the Master Chemical Mechanism, MCM v3 (Part A): tropospheric degradation of non-aromatic volatile organic compounds, Atmos Chem Phys, 3, 161-180, DOI 10.5194/acp-3-161-2003, 2003.

Schwantes, R. H., Teng, A. P., Nguyen, T. B., Coggon, M. M., Crounse, J. D., St Clair, J. M., Zhang, X., Schilling, K. A., Seinfeld, J. H., and Wennberg, P. O.: Isoprene NO3 Oxidation Products from the RO2 + HO2 Pathway, J Phys Chem A, 119, 10158-10171, 10.1021/acs.jpca.5b06355, 2015.

Seinfeld, J. H., and Pandis, S. N.: Atmospheric chemistry and physics : from air pollution to climate change, 2016.

Shilling, J. E., Zaveri, R. A., Fast, J. D., Kleinman, L., Alexander, M. L., Canagaratna, M. R., Fortner, E., Hubbe, J. M., Jayne, J. T., Sedlacek, A., Setyan, A., Springston, S., Worsnop, D. R., and Zhang, Q.: Enhanced SOA formation from mixed anthropogenic and biogenic emissions during the CARES campaign, Atmos Chem Phys, 13, 2091-2113, 10.5194/acp-13-2091-2013, 2013.

Shrivastava, M., Andreae, M. O., Artaxo, P., Barbosa, H. M. J., Berg, L. K., Brito, J., Ching, J., Easter, R. C., Fan, J. W., Fast, J. D., Feng, Z., Fuentes, J. D., Glasius, M., Goldstein, A. H., Alves, E. G., Gomes, H., Gu, D., Guenther, A., Jathar, S. H., Kim, S., Liu, Y., Lou, S. J., Martin, S. T., McNeill, V. F., Medeiros, A., de Sa, S. S., Shilling, J. E., Springston, S. R., Souza, R. A. F., Thornton, J. A., Isaacman-VanWertz, G., Yee, L. D., Ynoue, R., Zaveri, R. A., Zelenyuk, A., and Zhao, C.: Urban pollution greatly enhances formation of natural aerosols over the Amazon rainforest, Nat Commun, 10, ARTN 1046, 10.1038/s41467-019-08909-4, 2019.

Slade, J. H., de Perre, C., Lee, L., and Shepson, P. B.: Nitrate radical oxidation of gamma-terpinene: hydroxy nitrate, total organic nitrate, and secondary organic aerosol yields, Atmos Chem Phys, 17, 8635-8650, 10.5194/acp-17-8635-2017, 2017.

Song, M., Marcolli, C., Krieger, U. K., Zuend, A., and Peter, T.: Liquid-liquid phase separation in aerosol particles: Dependence on O:C, organic functionalities, and compositional complexity, Geophys Res Lett, 39, 10.1029/2012gl052807, 2012.

Spittler, M., Barnes, I., Bejan, I., Brockmann, K. J., Benter, T., and Wirtz, K.: Reactions of NO3 radicals with limonene and alpha-pinene: Product and SOA formation, Atmos Environ, 40, S116-S127, 10.1016/j.atmosenv.2005.09.093, 2006.

Spracklen, D. V., Jimenez, J. L., Carslaw, K. S., Worsnop, D. R., Evans, M. J., Mann, G. W., Zhang, Q., Canagaratna, M. R., Allan, J., Coe, H., McFiggans, G., Rap, A., and Forster, P.: Aerosol mass spectrometer constraint on the global secondary organic aerosol budget, Atmos Chem Phys, 11, 12109-12136, 10.5194/acp-11-12109-2011, 2011.

Stark, H., Yatavelli, R. L. N., Thompson, S. L., Kang, H., Krechmer, J. E., Kimmel, J. R., Palm, B. B., Hu, W. W., Hayes, P. L., Day, D. A., Campuzano-Jost, P., Canagaratna, M. R., Jayne, J. T., Worsnop, D. R., and Jimenez, J. L.: Impact of Thermal Decomposition on Thermal Desorption Instruments: Advantage of Thermogram Analysis for Quantifying Volatility Distributions of Organic Species, Environ Sci Technol, 51, 8491-8500, 10.1021/acs.est.7b00160, 2017.

Surratt, J. D., Gomez-Gonzalez, Y., Chan, A. W. H., Vermeylen, R., Shahgholi, M., Kleindienst, T. E., Edney, E. O., Offenberg, J. H., Lewandowski, M., Jaoui, M., Maenhaut, W., Claeys, M., Flagan, R. C., and Seinfeld, J. H.: Organosulfate formation in biogenic secondary organic aerosol, J Phys Chem A, 112, 8345-8378, 10.1021/jp802310p, 2008.

941 Takeuchi, M., and Ng, N. L.: Organic Nitrates and Secondary Organic Aerosol (SOA) Formation from
942 Oxidation of Biogenic Volatile Organic Compounds, Acs Sym Ser, 1299, 105-125, 2018.

943 Wangberg, I., Barnes, I., and Becker, K. H.: Product and mechanistic study of the reaction of NO3 radicals
944 with alpha-pinene, Environ Sci Technol, 31, 2130-2135, DOI 10.1021/es960958n, 1997.

945 Wayne, R. P., Barnes, I., Biggs, P., Burrows, J. P., Canosamas, C. E., Hjorth, J., Lebras, G., Moortgat, G.
946 K., Perner, D., Poulet, G., Restelli, G., and Sidebottom, H.: The Nitrate Radical - Physics, Chemistry, and
947 the Atmosphere, Atmos Environ a-Gen, 25, 1-203, Doi 10.1016/0960-1686(91)90192-A, 1991.

948 Weber, R. J., Sullivan, A. P., Peltier, R. E., Russell, A., Yan, B., Zheng, M., de Gouw, J., Warneke, C.,
949 Brock, C., Holloway, J. S., Atlas, E. L., and Edgerton, E.: A study of secondary organic aerosol formation
950 in the anthropogenic-influenced southeastern United States, J Geophys Res-Atmos, 112, Artn D13302,
951 10.1029/2007jd008408, 2007.

952 Xu, L., Guo, H. Y., Boyd, C. M., Klein, M., Bougiatioti, A., Cerully, K. M., Hite, J. R., Isaacman-VanWertz,
953 G., Kreisberg, N. M., Knote, C., Olson, K., Koss, A., Goldstein, A. H., Hering, S. V., de Gouw, J., Baumann,
954 K., Lee, S. H., Nenes, A., Weber, R. J., and Ng, N. L.: Effects of anthropogenic emissions on aerosol
955 formation from isoprene and monoterpenes in the southeastern United States (vol 112, pg 37, 2015), P Natl
956 Acad Sci USA, 112, E4509-E4509, 10.1073/pnas.1512279112, 2015a.

957 Xu, L., Suresh, S., Guo, H., Weber, R. J., and Ng, N. L.: Aerosol characterization over the southeastern
958 United States using high-resolution aerosol mass spectrometry: spatial and seasonal variation of aerosol
959 composition and sources with a focus on organic nitrates, Atmos Chem Phys, 15, 7307-7336, 10.5194/acp-
960 15-7307-2015, 2015b.

961 Xu, L., Pye, H. O. T., He, J., Chen, Y. L., Murphy, B. N., and Ng, N. L.: Experimental and model estimates
962 of the contributions from biogenic monoterpenes and sesquiterpenes to secondary organic aerosol in the
963 southeastern United States, Atmos Chem Phys, 18, 12613-12637, 10.5194/acp-18-12613-2018, 2018a.

964 Xu, L., Moller, K. H., Crounse, J. D., Otkjwr, R. V., Kjaergaard, H. G., and Wennberg, P. O.: Unimolecular
965 Reactions of Peroxy Radicals Formed in the Oxidation of alpha-Pinene and beta-Pinene by Hydroxyl
966 Radicals, J Phys Chem A, 123, 1661-1674, 10.1021/acs.jpca.8b11726, 2019.

967 Xu, W., Lambe, A., Silva, P., Hu, W. W., Onasch, T., Williams, L., Croteau, P., Zhang, X., Renbaum-
968 Wolff, L., Fortner, E., Jimenez, J. L., Jayne, J., Worsnop, D., and Canagaratna, M.: Laboratory evaluation
969 of species-dependent relative ionization efficiencies in the Aerodyne Aerosol Mass Spectrometer, Aerosol
970 Sci Tech, 52, 626-641, 10.1080/02786826.2018.1439570, 2018b.

971 Zare, A., Romer, P. S., Nguyen, T., Keutsch, F. N., Skog, K., and Cohen, R. C.: A comprehensive organic
972 nitrate chemistry: insights into the lifetime of atmospheric organic nitrates, Atmos Chem Phys, 18, 15419-
973 15436, 10.5194/acp-18-15419-2018, 2018.

974 Zhang, H. F., Yee, L. D., Lee, B. H., Curtis, M. P., Worton, D. R., Isaacman-VanWertz, G., Offenberg, J.
975 H., Lewandowski, M., Kleindienst, T. E., Beaver, M. R., Holder, A. L., Lonneman, W. A., Docherty, K. S.,
976 Jaoui, M., Pye, H. O. T., Hu, W. W., Day, D. A., Campuzano-Jost, P., Jimenez, J. L., Guo, H. Y., Weber,
977 R. J., de Gouw, J., Koss, A. R., Edgerton, E. S., Brune, W., Mohr, C., Lopez-Hilfiker, F. D., Lutz, A.,
978 Kreisberg, N. M., Spielman, S. R., Hering, S. V., Wilson, K. R., Thornton, J. A., and Goldstein, A. H.:
979 Monoterpenes are the largest source of summertime organic aerosol in the southeastern United States, P
980 Natl Acad Sci USA, 115, 2038-2043, 10.1073/pnas.1717513115, 2018.

Zhang, X., Cappa, C. D., Jathar, S. H., Mcvay, R. C., Ensberg, J. J., Kleeman, M. J., and Seinfeld, J. H.: Influence of vapor wall loss in laboratory chambers on yields of secondary organic aerosol, P Natl Acad Sci USA, 111, 5802-5807, 10.1073/pnas.1404727111, 2014.

Zhang, X., Schwantes, R. H., McVay, R. C., Lignell, H., Coggon, M. M., Flagan, R. C., and Seinfeld, J. H.: Vapor wall deposition in Teflon chambers, Atmos Chem Phys, 15, 4197-4214, 10.5194/acp-15-4197-2015, 2015.

Ziemann, P. J., and Atkinson, R.: Kinetics, products, and mechanisms of secondary organic aerosol formation, Chem Soc Rev, 41, 6582-6605, 10.1039/c2cs35122f, 2012.